

# FUNDAMENTALS OF DOSIMETRY BASED ON ABSORBED-DOSE STANDARDS

D.W.O. Rogers  
National Research Council of Canada  
e-mail: drogers@physics.carleton.ca (from 2003)  
WWW: <http://www.physics.carleton.ca/~drogers>

This chapter is the basis of a lecture given at the AAPM's 1996 Summer School in Vancouver, BC. It has been published by the AAPM in "Teletherapy Physics, Present and Future" edited by J. R. Palta and T. R. Mackie, pages 319 – 356 (AAPM, Washington DC, 1996).

David Rogers is now at the Physics Department of Carleton University, Ottawa, K1S 5B6.

## ABSTRACT

This chapter reviews the fundamentals of radiation dosimetry needed to do reference dosimetry for external beam radiotherapy when starting from an ion chamber calibrated in terms of absorbed-dose to water. It briefly reviews the status of primary standards for absorbed dose to water. The  $k_Q$  formalism developed to utilize these absorbed-dose calibration factors is described for use in electron and photon beams. In the ideal case, the needed  $k_Q$  factors are measured for each ion chamber and beam quality of interest in the clinic. Equations are developed for the factors needed to utilize this formalism in the proposed TG-51 dosimetry protocol of the AAPM. Special attention is paid to the issue of specifying beam quality in terms of percentage depth-dose at 10 cm for photon beams and  $R_{50}$  for electron beams. A proposal for using a reference depth of 0.6  $R_{50}$  – 0.1 cm in electron beam dosimetry is discussed. Factors needed for using plane-parallel chambers in a water phantom are also reviewed.

## Contents

<b>1. INTRODUCTION</b>	<b>3</b>
<b>2. STATUS OF ABSORBED-DOSE STANDARDS</b>	<b>3</b>
<b>3. FORMALISM USING ABSORBED-DOSE CALIBRATION FACTORS</b>	<b>4</b>
<b>4. ION CHAMBERS</b>	<b>5</b>
4.A. Theory . . . . .	5
4.A.1) Spencer-Attix Cavity Theory . . . . .	5
4.A.2) Handling Humidity Variation . . . . .	5
4.A.3) Cavity Theory with Corrections . . . . .	6
4.A.4) The Wall Correction Factor, $P_{\text{wall}}$ . . . . .	6
4.A.5) The Replacement Correction Factor, $P_{\text{repl}} = P_{\text{gr}}P_{\text{fl}}$ . . . . .	7
4.A.6) The Central Electrode Correction Factor, $P_{\text{cel}}$ . . . . .	9
4.B. Practical Considerations . . . . .	10
4.B.1) Correction for Ion Recombination, $P_{\text{ion}}$ . . . . .	10
4.B.2) Temperature and Pressure Corrections . . . . .	10
4.B.3) Waterproofing Sleeves . . . . .	10
<b>5. BEAM-QUALITY SPECIFICATION</b>	<b>11</b>
5.A. Why Do We Need to Specify Beam Quality? . . . . .	11
5.B. Specification of Photon Beam Quality . . . . .	11
5.C. Specification of Electron Beam Quality . . . . .	13
5.C.1) Determination of $R_{50}$ . . . . .	13

5.C.2)	The mean energy at the phantom surface, $\bar{E}_o$ . . . . .	14
5.C.3)	Problems with stopping-power ratios using mono-energetic beams . . . . .	15
5.C.4)	Direct use of $R_{50}$ as beam quality specifier . . . . .	15
<b>6.</b>	<b>VALUES OF <math>k_Q</math></b> . . . . .	<b>16</b>
6.A.	Calculation of $k_Q$ Values . . . . .	16
6.A.1)	An equation for $k_Q$ . . . . .	16
6.A.2)	Photon Beams . . . . .	16
6.A.3)	Electron Beams . . . . .	19
6.B.	Measurement of $k_Q$ Values . . . . .	22
<b>7.</b>	<b>SUMMARY</b> . . . . .	<b>23</b>
<b>8.</b>	<b>ACKNOWLEDGMENTS</b> . . . . .	<b>23</b>
<b>9.</b>	<b>REFERENCES</b> . . . . .	<b>23</b>

## 1. INTRODUCTION

Accurate measurement of the dose delivered to the tumor in external beam radiotherapy is one of the primary responsibilities of a medical physicist. In general, such measurements have been based on the use of ion chambers calibrated in terms of exposure or air kerma and the application of a dosimetry protocol such as the AAPM's TG-21 protocol (AAPM TG-21 1983; AAPM TG-21 1984; Schulz *et al* 1986) or the IAEA's Code of Practice (IAEA 1987). These protocols were a significant step forward since they provided a procedure which was capable of incorporating the correct physics. This came at the expense of considerable complexity. One manifestation of this complexity is a large number of small errors and inconsistencies in the TG-21 protocol which fortunately tend to cancel out (see *e.g.* my lecture at the previous summer school which dealt with many of these issues and gave a corrected derivation of the TG-21 protocol equations (Rogers 1992d)). However, even using the corrected protocols the overall uncertainty in the absorbed dose assigned under reference conditions is about 3 to 4% (all uncertainty estimates in this chapter are for one standard deviation, representing a confidence level of 68%). For extensive reviews of various dosimetry protocols see Nath and Huq (1995) and Andreo (1993).

Much of the complexity of the TG-21 and similar protocols comes from the fact that they start from an ion chamber calibrated free-in-air for one quantity, air kerma, and must transfer this information to obtain another quantity, absorbed dose to water, based on a measurement in a phantom. To overcome these complexities, primary standards laboratories have been developing standards for absorbed dose to water in photon beams from  $^{60}\text{Co}$  and accelerator beams (Rogers 1992b; Shortt *et al* 1993; Domen 1994; Boutillon *et al* 1994; Ross and Klassen 1996) and these have an uncertainty of 1% or less. Also, many improvements in radiation dosimetry have been made in the 15 years since TG-21 was developed. To make use of this greater accuracy and to incorporate these improvements, the AAPM has established a task group, TG-51, to develop a new external beam dosimetry protocol. There are several approaches which could be used, but after careful study it has been decided to base the new protocol on calibrating ion chambers in terms of absorbed dose to water in a  $^{60}\text{Co}$  beam.

In this chapter I will discuss the fundamentals of ion chamber dosimetry which underlie the approach being adopted by TG-51, with emphasis on various developments which have occurred in the last few years. However, this is a personal contribution and although I am on TG-51, this document does not represent the opinion of TG-51, nor does it present many of the details of the protocol since these are still evolving.

## 2. STATUS OF ABSORBED-DOSE STANDARDS

Three very different approaches have been used to provide standards for absorbed dose to water in photon beams. I reviewed these at the previous summer school (Rogers 1992b) and progress has continued since then. The most common approach is to use a graphite calorimeter to establish the absorbed dose to graphite and then use various procedures to infer the absorbed dose to water in the same beam (Pruitt *et al* 1981; Domen and Lamperti 1974). A second approach is to use the total absorption in Fricke solution of an electron beam of known energy and charge to calibrate the solution and then use the Fricke in a small vial to establish the dose at a point in a water phantom by assuming that the calibration of the Fricke solution (*i.e.*  $\epsilon G$ ) does not change with beam quality (Feist 1982). A third approach is to use water calorimetry, either to calibrate Fricke solution in the beam quality of interest (Ross *et al* 1984; Ross *et al* 1989) or use a small volume of sealed, high-purity water in a water phantom to do a direct measurement of the absorbed dose to water (Domen 1994; Seuntjens *et al* 1993). There has been a recent review of both forms of water calorimetry by Ross and Klassen (1996).

There have been several comparisons of the standards in different national standards laboratories and there is satisfactory agreement between the various methods at the 1% level or better (Boutillon *et al* 1994; Shortt *et al* 1993). An important point is that each of these three methods has different types of systematic uncertainties and thus the system of standards being developed is highly robust against systematic errors affecting all the standards. The situation for air-kerma standards is different since almost all the primary standards

in the world use the same basic approach (a graphite-walled cavity ion chamber) and thus comparisons between them cannot resolve systematic uncertainties in the technique itself. More specifically, there have been challenges to parts of the theory underlying the air-kerma standards and different approaches in establishing certain corrections lead to up to 1% differences in these standards, in particular between the Canadian and US standards (Bielajew and Rogers 1992).

In summary, there is a robust system of absorbed dose to water standards in place in primary standards laboratories. These standards are capable of measuring the absorbed dose not only in  $^{60}\text{Co}$  beams but in accelerator beams.

### 3. FORMALISM USING ABSORBED-DOSE CALIBRATION FACTORS

Given the existence of the high quality primary standards for absorbed dose to water and the fact that the absorbed dose to water is the quantity which is used for reference dosimetry in radiotherapy, it makes sense to base clinical dosimetry on absorbed-dose calibration factors for ion chambers. Ion chambers are used because high-quality chambers are available for reasonable cost, they have the capability of making precise and stable measurements in radiation fields encountered in the clinic, and the theory for interpreting their output is reasonably well understood. In the last few years a formalism for such a process has been widely discussed (Hohlfeld 1988; ICRU 1990; Rogers 1992c; Andreo 1992; Rogers *et al* 1994) and has been adopted for TG-51.

One starts with an absorbed-dose to water calibration factor,  $N_{\text{D,w}}^{\text{Q}}$ , defined by:

$$D_{\text{w}}^{\text{Q}} = MP_{\text{ion}}N_{\text{D,w}}^{\text{Q}} \quad [\text{Gy}] \quad (1)$$

where  $D_{\text{w}}^{\text{Q}}$  is the absorbed-dose to water (in Gy) at the point of measurement of the ion chamber in the absence of the chamber (the center of a cylindrical chamber and the front of the air cavity in a plane-parallel ion chamber),  $M$  is the temperature and pressure corrected (see section 4.B.2) electrometer reading in coulombs (C) or meter units (rdg),  $P_{\text{ion}}$  corrects for ion chamber collection efficiency not being 100% (see section 4.B.1), and  $N_{\text{D,w}}^{\text{Q}}$  is the absorbed-dose to water calibration factor (in Gy/C or Gy/rdg) for the ion chamber when placed under reference conditions in a beam of quality  $Q$ . In North America the calibration factor applies under reference conditions of temperature, pressure and humidity, *viz.* 22°C, 101.3 kPa and relative humidity between 20 and 80%. Note that because it can become significant in accelerator beams, the inclusion of  $P_{\text{ion}}$  in eq.(1) is different from previous North American practice for air-kerma or exposure calibration factors where ion recombination effects were part of the calibration factor, *i.e.* the exposure,  $X$ , is given by:  $X = MN_{\text{X}}$  where  $N_{\text{X}}$  is the exposure calibration factor.

Clearly the most direct method of clinical dosimetry is to get an ion chamber calibrated for each beam quality  $Q$  needed for a clinic and then apply eq.(1). Since this would both be very expensive (it requires an accelerator for the calibration) and available at very few places (the ADCL's do not have accelerators of their own), it is easier to start from an absorbed-dose calibration factor for a  $^{60}\text{Co}$  beam, *viz.*  $N_{\text{D,w}}^{60\text{Co}}$ . In this case, define a factor  $k_{\text{Q}}$  such that:

$$N_{\text{D,w}}^{\text{Q}} = k_{\text{Q}}N_{\text{D,w}}^{60\text{Co}}, \quad [\text{Gy}] \quad (2)$$

*i.e.*  $k_{\text{Q}}$  converts the absorbed-dose calibration factor for a  $^{60}\text{Co}$  beam into a calibration factor for an arbitrary beam quality  $Q$ . In general, the value of  $k_{\text{Q}}$  is chamber specific. Using  $k_{\text{Q}}$ , gives:

$$D_{\text{w}}^{\text{Q}} = MP_{\text{ion}}k_{\text{Q}}N_{\text{D,w}}^{60\text{Co}} \quad [\text{Gy}]. \quad (3)$$

In an ideal world, values of  $k_{\text{Q}}$  measured using primary standards for absorbed dose would be available for all the ion chambers used for reference dosimetry. Such a project is underway at NRCC for accelerator photon beams for many widely used Farmer-like ion chambers, but equivalent data will not be available

for all chambers, nor for electron beams in the foreseeable future. Thus it is important to have ways of calculating  $k_Q$ , and this is discussed below after a review of the necessary fundamentals.

## 4. ION CHAMBERS

### 4.A. Theory

#### 4.A.1) Spencer-Attix Cavity Theory

The central theory underlying ion chamber dosimetry is Spencer-Attix cavity theory(1955) which relates the dose delivered to the gas in the ion chamber,  $D_{\text{gas}}$ , to the dose in the surrounding medium,  $D_{\text{med}}$  by the relationship:

$$D_{\text{med}} = D_{\text{gas}} \left( \frac{\bar{L}}{\rho} \right)_{\text{gas}}^{\text{med}}, \quad (4)$$

where the stopping-power ratio,  $\left( \frac{\bar{L}}{\rho} \right)_{\text{gas}}^{\text{med}}$ , is the ratio of the spectrum averaged mass collision stopping powers for the medium to that for the gas where the averaging extends from a minimum energy  $\Delta$  to the maximum electron energy in the spectrum. The fundamental assumptions of this theory are that: i) the cavity does not change the electron spectrum in the medium; ii) all the dose in the cavity comes from electrons entering the cavity, *i.e.* they are not created in the cavity; and iii) electrons below the energy  $\Delta$  are in charged particle equilibrium. Unlike Bragg-Gray cavity theory, Spencer-Attix theory applies where charged particle equilibrium of the *knock-on* electrons above  $\Delta$  does not exist, which is generally the case near an interface between media or at the edge of a beam.

There is an extensive literature on the Monte Carlo calculation of stopping-power ratios (Nahum 1978; Andreo and Brahme 1986; ICRU 1984a; Ding *et al* 1995) and there is agreement between various calculations at about the 0.1% level if the same stopping power data are used. However, there has been considerable confusion caused by the use of a variety of different electron stopping power-data sets in earlier protocols (see, *e.g.* Rogers *et al* (1986)). There is now a consensus to use the stopping-power data from ICRU Report 37 (1984b) (based on the work of Berger and Seltzer at NIST(1983)) and they are used exclusively here. The TG-21 protocol used these data for electron beams but used an earlier set (which differed by over 1% in places) for the photon beam data.

#### 4.A.2) Handling Humidity Variation

To make use of eq.(4) requires a connection between  $D_{\text{gas}}$  and the charge measured from the ion chamber. If  $M'$  is the charge released in the ion chamber, then:

$$D_{\text{gas}} = \left( \frac{W}{e} \right)_{\text{gas}} \frac{M'}{m_{\text{gas}}} \quad (\text{Gy}), \quad (5)$$

where  $\left( \frac{W}{e} \right)_{\text{gas}}$  gives the energy deposited in a gas per unit charge released, and fortunately for ion chamber dosimetry, is a constant for dry air, independent of electron energy (*viz.*  $33.97 \pm 0.05 \text{ JC}^{-1}$  Boutillon and Perroche-Roux (1987)), and  $m_{\text{gas}}$  is the mass of the gas in the cavity. One complication in ion chamber dosimetry is that the humidity in the air causes each of the quantities  $\left( \frac{W}{e} \right)_{\text{gas}}$ ,  $m_{\text{gas}}$  and  $\left( \frac{\bar{L}}{\rho} \right)_{\text{gas}}^{\text{w}}$  to vary by anywhere up to 1%. This has caused considerable unnecessary confusion in the TG-21 protocol (see Rogers and Ross (1988) and Mijnheer and Williams (1985) and references therein for a complete discussion). To handle these variations, one defines a humidity correction factor:

$$K_{\text{h}} = \left( \frac{W}{e} \right)_{\text{air}}^{\text{gas}} \frac{m_{\text{air}}}{m_{\text{gas}}} \left( \frac{\bar{L}}{\rho} \right)_{\text{gas}}^{\text{air}}, \quad (6)$$

which has the feature of being equal to 0.997 for relative humidity between roughly 15% and 80%. Multiplying the right side of eq.(5) by  $K_h$  and inserting the results into eq.(4) leads to the following simplifications:

$$D_{\text{med}} = D_{\text{air}} \left( \frac{\bar{L}}{\rho} \right)_{\text{air}}^{\text{med}} \quad (\text{Gy}), \quad (7)$$

$$D_{\text{air}} = K_h \left( \frac{W}{e} \right)_{\text{air}} \frac{M'}{m_{\text{air}}} \quad (\text{Gy}) \quad (8)$$

where eq.(7) has made use of the fact that  $(\bar{L}/\rho)_{\text{gas}}^{\text{med}} (\bar{L}/\rho)_{\text{air}}^{\text{gas}} = (\bar{L}/\rho)_{\text{air}}^{\text{med}}$ . Note that all the references are now to dry air, except for  $M'$ . The charge released,  $M'$ , is related to the measured charge below (section 4.B.1).

#### 4.A.3) Cavity Theory with Corrections

Unfortunately, real ion chambers are not ideal cavities. The first issue that this raises is where the cavity is measuring the dose, a complex problem which is discussed below (section 4.A.5). However, for a cylindrical ion chamber, in-phantom calibration factors apply with the central axis of the chamber at the point of measurement, and for plane-parallel chambers, the point of measurement is taken as the inside face of the front window. There are also several correction factors, as given in eq.(9) which are needed before applying eq.(4), *viz.*:

$$D_{\text{med}} = D_{\text{air}} \left( \frac{\bar{L}}{\rho} \right)_{\text{air}}^{\text{med}} P_{\text{wall}} P_{\text{fl}} P_{\text{gr}} P_{\text{cel}}. \quad (9)$$

These correction factors are discussed briefly below but for an extensive review of these issues, see Nahum (1994).

#### 4.A.4) The Wall Correction Factor, $P_{\text{wall}}$

The  $P_{\text{wall}}$  correction in eq.(9) accounts for the fact that the wall and other parts of the chamber are not usually made of the same material as the medium. This factor is designated  $P_{\text{wall}}$ .

In **electron** beams,  $P_{\text{wall}}$  has traditionally been assumed to be 1.00. Nahum (1988) has developed a theoretical model of the effect of the wall material on the electron spectrum in the cavity. It qualitatively agrees with the experimental data in an extreme case. Based on this model, Nahum has shown that the wall effect in electron beams due to changes in the spectrum, should be less than 1%, and usually much less for situations of importance in clinical dosimetry. More recently, Klevenhagen (1991) and Hunt *et al* (1988) have pointed out that for plane-parallel chambers, the electron backscatter from non-water materials behind the air cavity is different from that of water and this induces a change in the ion chamber reading. This should, in principle, be corrected for using the  $P_{\text{wall}}$  correction given in table 1. The corrections can be substantial for low-energy beams. Preliminary results of Monte Carlo calculations of this effect for the entire chamber for NACP and PTW/Markus chambers also indicate an effect of the order of 1 or 2% (Ma and Rogers 1995).

In **photon** beams, the correction factor for the wall effect in the case of a chamber with a waterproofing sheath, is given by a formula based on a slight extension of the work of Shiragai (1978) and (1979):

$$P_{\text{wall}} = \frac{1}{\left( \frac{\bar{L}}{\rho} \right)_{\text{air}}^{\text{med}} \left[ \alpha \left( \frac{\bar{L}}{\rho} \right)_{\text{wall}}^{\text{air}} \left( \frac{\mu_{\text{en}}}{\rho} \right)_{\text{med}}^{\text{wall}} + \tau \left( \frac{\bar{L}}{\rho} \right)_{\text{sheath}}^{\text{air}} \left( \frac{\mu_{\text{en}}}{\rho} \right)_{\text{med}}^{\text{sheath}} + (1 - \alpha - \tau) \left( \frac{\bar{L}}{\rho} \right)_{\text{med}}^{\text{air}} \right]}, \quad (10)$$

where  $\left( \frac{\mu_{\text{en}}}{\rho} \right)_{\text{B}}^{\text{A}}$  is the ratio of mass energy absorption coefficients for material A to material B (relating the doses in these materials under charged particle equilibrium in a photon beam);  $\alpha$  is the fraction of ionization

Table 1:  $P_{\text{wall}}$  correction factor for plane-parallel chambers with effectively thick back walls of the materials shown. Data from Klevenhagen (1991), based on the results of Hunt *et al* (1988).

$\bar{E}_z$ , energy at depth of chamber(MeV)	Graphite	PMMA	Polystyrene
3	1.010	1.012	1.021
4	1.009	1.011	1.018
6	1.006	1.008	1.013
10	1.004	1.005	1.009
14	1.003	1.003	1.006
20	1.001	1.001	1.002

in the cavity due to electrons from the chamber wall;  $\tau$  is the fraction of ionization in the cavity due to electrons from the waterproofing sheath and  $(1 - \alpha - \tau)$  is the fraction due to electrons from the phantom. There are data available in the TG-21 protocol for the various parameters needed as a function of beam quality, including  $\alpha$  and  $\tau$  based on the measurements of Lempert *et al* (1983) (which I have verified using Monte Carlo calculations, unpublished). This correction is typically 1% or less for most ion chambers but the accuracy of the formula has not been rigorously demonstrated and there are indications that there are problems with it (Hanson and Tinoco 1985; Gillin *et al* 1985; Ross *et al* 1994). There are also conceptual problems with the correction factor since it uses many inaccurate assumptions in its derivation and ignores changes in attenuation and scatter by the wall. For a complete discussion and derivation of the  $P_{\text{wall}}$  equation, see Rogers (1992d) or Nahum (1994). Note that eq.(10) differs in form from that associated with the TG-21 protocol, but has the same numerical values in practice.

#### 4.A.5) The Replacement Correction Factor, $P_{\text{repl}} = P_{\text{gr}}P_{\text{fl}}$ .

The insertion of a cavity into a medium causes changes in the electron spectrum and the replacement correction factor,  $P_{\text{repl}}$ , accounts for these changes.  $P_{\text{repl}}$  can be thought of as having two components, the gradient and fluence correction factors:

$$P_{\text{repl}} = P_{\text{gr}}P_{\text{fl}}. \quad (11)$$

#### The Gradient Correction Factor, $P_{\text{gr}}$ .

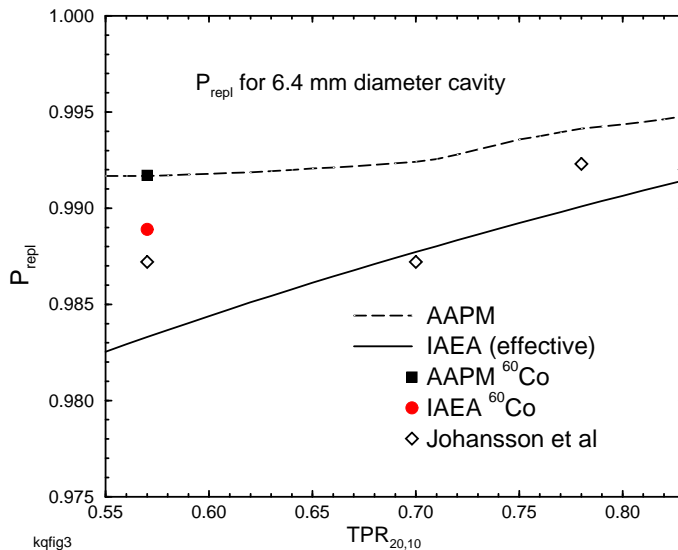
One effect of the cavity is, in essence, to move the point of measurement upstream from the center of the chamber. The electron fluence in the cavity is representative of the fluence in the medium at some point closer to the source because there is less attenuation or buildup in the cavity than in the medium. This component of  $P_{\text{repl}}$  is called **the gradient correction**,  $P_{\text{gr}}$ , because its magnitude depends on the dose gradient at the point of measurement. For cylindrical chambers, these corrections depend on the gradient of the dose and on the inner diameter of the ion chamber. The steeper the gradient, the larger the correction. Also, the larger the radius, the larger the correction. For plane-parallel chambers in photon or electron beams, the point of measurement at the front of the air cavity is already thought to take into account any gradient effects and hence there is no need for a  $P_{\text{gr}}$  correction, even in regions with a gradient.

In **electron** beams, for measurements at  $d_{\text{max}}$  where the gradient of the dose is zero,  $P_{\text{gr}} = 1.00$ , but for measurements away from  $d_{\text{max}}$ ,  $P_{\text{gr}}$  becomes important for cylindrical chambers, especially for low-energy beams where there are steep gradients.

For **photons**, gradient correction factors in various protocols are based on different sources. TG-21 based its values on the work of Cunningham and Sontag (1980) which is a mixture of experiment and mostly calculations. Many other protocols have used the measured data of Johansson *et al* (1977) but as shown in figure 1 there are considerable differences amongst the original data, the TG-21 data and what is recommended in the IAEA Code of Practice (1987).

It is clear that the gradient correction factor represents a significant uncertainty in present dosimetry pro-

Figure 1: Value of  $P_{\text{repl}}$  ( $= P_{\text{gr}}$  in a photon beam), for a 6.4 mm cavity, as a function of beam quality specified by  $\text{TPR}_{10}^{20}$ . The AAPM values are from TG-21, based on the calculations of Cunningham and Sontag (1980). The IAEA values are the effective values (determined as described in Rogers (1992c)) corresponding to the offsets used by the IAEA Code of Practice (1987), which were nominally based on the work of Johansson *et al* (1977) which is shown as diamonds.



ocols. It is also worth noting that another way to correct for the gradient is used by the IAEA Code of Practice (1987), *viz.* the effective point of measurement approach. This same approach is recommended for measuring depth-dose or depth-ionization curves by the AAPM's TG-25 on electron beam dosimetry (Khan *et al* 1991). The method treats the point of measurement as being slightly up-stream of the center of the ion chamber. For electron beams, both groups recommend an offset of  $0.5r$  where  $r$  is the radius of the cylindrical chamber's cavity and for photon beams the shift correction is  $0.75r$ . It must be emphasized that if one is using a  $P_{\text{repl}}$  value in photon beams for reference dosimetry, then the effective point of measurement of a cylindrical chamber must be taken as its center.

### The Fluence Correction Factor, $P_{\text{fl}}$ .

The other component of  $P_{\text{repl}}$  is the fluence correction,  $P_{\text{fl}}$ , which corrects for other changes in the electron fluence spectrum due to the presence of the cavity. Corrections for changes in the electron fluence are only needed if the ion chamber is in a region where full or transient charged particle equilibrium has not been established, *i.e.* in the buildup region or near the boundaries of a photon beam or anywhere in an electron beam.

Fluence corrections **are not required** for **photon** dose determinations made at or beyond  $d_{\text{max}}$  in a broad beam because transient electron equilibrium exists. The Fano theorem tells us that under conditions of charged particle equilibrium the electron spectrum is independent of the density in the medium (see p 255, Attix (1986)). To the extent that the cavity gas is just low-density medium material, this theorem tells us that the electron fluence spectrum is not affected by the cavity except in the sense of the gradient correction discussed above, which in essence accounts for there being transient rather complete charged particle equilibrium. Hence no fluence correction factor is needed in regions of transient charged particle equilibrium.

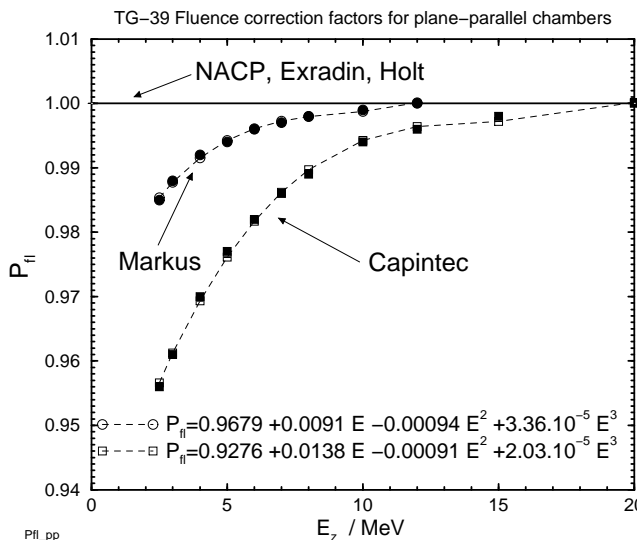
In **electron** beams there are two competing effects. The **in-scatter effect** which increases the fluence in the cavity because electrons are not scattered out by the gas and the **obliquity effect** which decreases the fluence in the cavity because the electrons go straight instead of scattering. The in-scatter effect tends to dominate, especially at low energies and  $P_{\text{fl}}$  can be up to 5% less than unity for cylindrical chambers at  $d_{\text{max}}$  in electron beams. TG-21 tabulates recommended values for cylindrical chambers as a function of the mean energy of the electrons at the point of measurement and recent measurements have confirmed these values for a Farmer-like ion chamber (Van der Plaetsen *et al* 1994). The fluence effect is so large at low energies that it becomes important to use plane-parallel chambers for these beams since  $P_{\text{fl}}$  has been shown to be unity for well-guarded plane-parallel chambers (Mattsson *et al* 1981; Van der Plaetsen *et al* 1994). However, the AAPM's TG-39 on the calibration of plane-parallel chambers (Almond *et al* 1994) has recommended non-unity values of  $P_{\text{fl}}$  for both the Markus and Capintec plane-parallel chambers (see fig 2).

Table 2:  $P_{cel}$  correction factor required for farmer-like chambers with an aluminum electrode of 1 mm diameter, based on the calculations of Ma and Nahum (1993). Factors apply past  $d_{max}$  in photon beams and near  $d_{max}$  or  $0.6 R_{50} - 0.1$  cm in electron beams. The  $\%dd(10)_x$  values exclude electron contamination (see section 5.B.). Note that  $P_{cel}$  as defined here is consistent with the other correction factors but is not the same as the IAEA’s global  $P_{cel}$  correction.

NAP/MeV	Beam Quality		$P_{cel}$
	TPR <sub>10</sub> <sup>20</sup>	$\%dd(10)_x$	
photons			
<sup>60</sup> Co	0.58	56%	0.9926(15)
4MV	0.62	62%	0.9935(7)
6MV	0.67	67%	0.9930(11)
10MV	0.73	72%	0.9945(9)
15MV	0.76	78%	0.9955(16)
24MV	0.80	86%	0.9957(9)
electrons			
<13 MeV			1.000
≥13 MeV			0.998

All the recommended values of  $P_{fl}$  apply ONLY at  $d_{max}$  since that is where they were measured (Johansson

Figure 2: The  $P_{fl}$  factors for plane-parallel chambers recommended by TG-39 (Almond *et al* 1994) plus cubic fits to the curves for the Markus and Capintec chambers. The factors are given as a function of  $\bar{E}_z$  (E in the figure), the mean energy at the depth of measurement.



*et al* 1977; Van der Plaetsen *et al* 1994) and strictly speaking, they are not appropriate for corrections of depth-dose curves as sometimes suggested (*e.g.* Khan (1991)), although this is probably better than making no correction.

4.A.6) The Central Electrode Correction Factor,  $P_{cel}$

Cylindrical chambers have central electrodes in their cavities and these have some effect on the chamber response. For electrodes made out of the same material as the phantom, any effect of the electrode is properly part of  $P_{fl}$ . Any further effects due to the electrode being made of another material is properly part of  $P_{wall}$  but it is useful to separate out this effect and call it  $P_{cel}$  if the electrode material is different from the wall material. The effect is non-negligible for those widely used chambers which have aluminum electrodes to give a flat energy response in low-energy x-ray fields (*e.g.* many NEL and PTW chambers). A set of highly precise Monte Carlo calculations has been reported (Ma and Nahum 1993). The first important result of that work is that 1 mm graphite electrodes have no effect on the response in a water phantom (as expected since  $P_{fl}$  is unity in photon beams and the difference between a water and graphite electrode should be negligible). In electron beams the effects are also small (<0.2%) and are in principle included in  $P_{fl}$  and/or  $P_{wall}$ . However, for 1 mm diameter aluminum electrodes the effect in photon beams is an increase in response by 0.43 to 0.75%, requiring the correction factors in table 2. These data can be generated and

extrapolated using:

$$P_{\text{cel}} = 0.9862 + 0.000112(\%dd(10)_x). \quad (12)$$

The effects in electron beams are quite small and vary with depth. However, the effect on dosimetry in electron beams is actually larger than in photon beams because, in essence, the final dose is multiplied by  $P_{\text{cel}}(e^-)/P_{\text{cel}}(^{60}\text{Co})$  and the factor in the denominator is quite large (see section 6.A.3).

## 4.B. Practical Considerations

### 4.B.1) Correction for Ion Recombination, $P_{\text{ion}}$

In general, ion chambers do not collect all the charge released in the air cavity and the factor  $P_{\text{ion}}$  corrects for this lack of 100% charge collection.

$$M' = MP_{\text{ion}} \quad [\text{C or rdg}], \quad (13)$$

where  $M'$  is the charge released in the ion chamber and  $M$  is the charge collected. This correction is fairly well understood (see the review by Boag (1987)) and there is a standard technique for evaluating the correction which involves measuring the charge collected at 2 voltages and then determining the correction required (see Weinhaus and Meli (1984)). Although the TG-21 protocol recommended a voltage ratio of 2 for these measurements, the underlying theory requires a ratio of 2.5 or more.

Although this correction is reasonably well understood, ion chambers with large correction factors (say  $>2\%$  correction), should probably not be used since the uncertainty in the correction may become unacceptable.

It must be emphasized that this correction depends on the dose to the air in the ion chamber **per pulse**. Thus, if either the dose rate or the pulse rate at a constant dose rate are varied, then  $P_{\text{ion}}$  must be re-evaluated. This variation would even affect measurement of a depth-dose curve if an instrument with a large value of  $P_{\text{ion}}$  was being used.

### 4.B.2) Temperature and Pressure Corrections

Temperature and pressure variations affect the mass of air inside an ion chamber. Since the total charge produced depends on the product of the dose to the gas and the mass of the gas (eq.(5), it also depends on the temperature and pressure. Since ion chambers are all calibrated under standard conditions of temperature and pressure, *i.e.* for a given mass of air in them, it is essential to normalize all readings of ion chamber charge back to these same reference conditions ( $T_o = 22^\circ\text{C}$  and pressure at  $P_o = 101.33 \text{ kPa}$ , 1 atmosphere). This is done using:

$$M = M_o \frac{101.33}{P} \times \frac{T + 273.2}{273.2 + 22.0} \quad [\text{C or rdg}], \quad (14)$$

where  $M$  is the corrected reading,  $M_o$  is the uncorrected reading,  $T$  is the temperature in degrees celsius and  $P$  is the pressure in kilopascals (not corrected to sea level).

### 4.B.3) Waterproofing Sleeves

Since the protocol will require absorbed-dose calibration factors measured in a water phantom and also clinical measurements in water, the issue of how to waterproof the chamber becomes important. There are already good chambers on the market which are waterproof. This seems like a desirable goal. But for chambers that are not, a waterproofing sleeve will be required. In eq.(10) there is an explicit term for a waterproofing sleeve but as mentioned, the experimental data are not in particularly good agreement with the theory (Hanson and Tinoco 1985; Gillin *et al* 1985; Ross and Shortt 1992). For sufficiently thin sleeves of PMMA ( $< 1 \text{ mm}$ ) or latex rubber, the experimental data show that there is less than a 0.2% effect on the chamber response which varies little with beam quality and thus can be ignored. The various calibration laboratories are working on a calibration protocol which will incorporate the need for such a sleeve.

## 5. BEAM-QUALITY SPECIFICATION

### 5.A. Why Do We Need to Specify Beam Quality?

Clinically one must be able to identify accelerator beams for many reasons, and usually just referring to the 12 MV beam or the 18 MeV beam is adequate. However, for reference dosimetry we need more precise specification of the beam quality,  $Q$ , so that one can select the correct value of  $k_Q$  in the dose equation, eq.(3). As is shown below in fig. 9 and eq.(26), the value of  $k_Q$  is dominated by the water to air stopping-power ratio which varies by over 15% in clinical beams (from 1.13 for  $^{60}\text{Co}$  beams to 0.98 for 50 MeV electron beams).

### 5.B. Specification of Photon Beam Quality

The TG-21 protocol uses the quantity  $\text{TPR}_{10}^{20}$  to specify photon beam quality when selecting  $(\bar{L}/\rho)_{\text{air}}^w$  although it also uses the nominal accelerating potential (NAP) to specify other, less sensitive quantities. The value of  $\text{TPR}_{10}^{20}$  is determined by measuring the absorbed dose or ionization on the beam-axis at depths of 20 cm and 10 cm for a constant source-detector distance and a 10 cm x 10 cm field at the plane of the chamber (*i.e.* one must move the phantom, or at least its surface).

The idea of using measured ratios of ionization or dose at two depths was first introduced in the Nordic dosimetry protocol to specify the accelerator energy (NACP 1980). The TG-21 protocol goes one step further and directly associates the beam quality index with the stopping-powers ratios needed. This is based on the work of Cunningham and Schulz (1984) who found a universal curve relating these two quantities based on analytic calculations of stopping-power ratios and  $\text{TPR}_{10}^{20}$  for a variety of clinical photon spectra. Andreo and Brahme (1986) showed that for clinical photon spectra one could accurately calculate values of  $\text{TPR}_{10}^{20}$  using Monte Carlo techniques and found a curve relating stopping-power ratios for clinical beams and  $\text{TPR}_{10}^{20}$ . They also showed that for a given NAP there are up to 1.3% variations in the stopping-power ratio. It is for this reason that  $\text{TPR}_{10}^{20}$  is used rather than NAP. However,  $\text{TPR}_{10}^{20}$  is also not an ideal beam quality specifier because there are variations of over 1% in the stopping-power ratio associated with beams of the same  $\text{TPR}_{10}^{20}$  (see fig 3). Since eq.(25) below shows  $N_{D,w}^Q$  is directly proportional to the stopping-power ratio, this can be a problem for standards laboratories since their beams might not match those in the clinic, and hence the value of  $N_{D,w}^Q$  might not apply in the clinic for a beam of the same  $\text{TPR}_{10}^{20}$ .

As seen in fig. 3, high-energy photon beams also lead to other problems with  $\text{TPR}_{10}^{20}$  as a beam specifier. The high-energy swept beams from the racetrack microtron accelerators have considerably different curves of stopping-power ratios *vs*  $\text{TPR}_{10}^{20}$  values compared to other “typical clinical beams”. Furthermore, for high-energy beams,  $\text{TPR}_{10}^{20}$  is an insensitive quality specifier. For example a 1% change in  $\text{TPR}_{10}^{20}$  for values near 0.8 leads to a 3 MV change in the nominal accelerating potential (near 20 MV) and a 0.4% change in the water to air stopping-power ratio. In contrast, for values of  $\text{TPR}_{10}^{20}$  near 0.7 a 1% change corresponds to a 0.1% change in stopping-power ratio and only an 0.5 MV change in the NAP.

Manufacturers and others have often specified beam quality in terms of an NAP in MV which is not well defined. The obvious definition in terms of the energy of the electrons from the accelerator is not very useful because this energy is usually not well known. More importantly, the beam quality is strongly affected by the type of beam flattening used (see LaRiviere (1989) and references therein for a good discussion). LaRiviere proposed that the beam quality in MV should be specified in terms of %dd(10), the measured percentage depth dose at 10 cm depth in a  $10 \times 10 \text{ cm}^2$  field at a source to surface distance (SSD) of 100 cm with

$$Q = 10^{[\%dd(10) - 46.78]/26.09} \quad [\text{MV}], \quad (15)$$

which is a good fit to the “experimental” data although there is scatter in the initial data caused by the lack of a clear definition of  $Q$ .

Kosunen and Rogers (1993) took LaRiviere’s argument one step further and showed that for any bremsstrahlung beam above 4MV, one has a linear relationship between stopping-power ratio and %dd(10)<sub>x</sub>

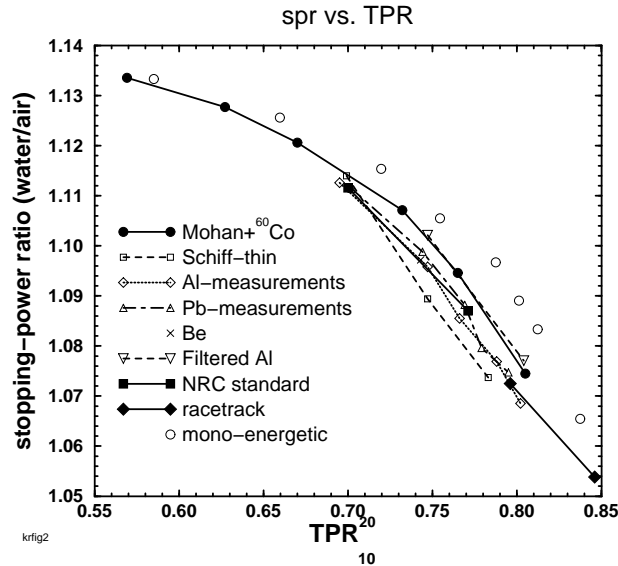


Figure 3: Water to air stopping-power ratios  $vs$   $TPR_{10}^{20}$  for nine families of photon spectra, demonstrating variations when using  $TPR_{10}^{20}$  as a beam quality specifier. Flattened, *i.e.* practical beams are shown as closed symbols. From Kosunen and Rogers (1993).

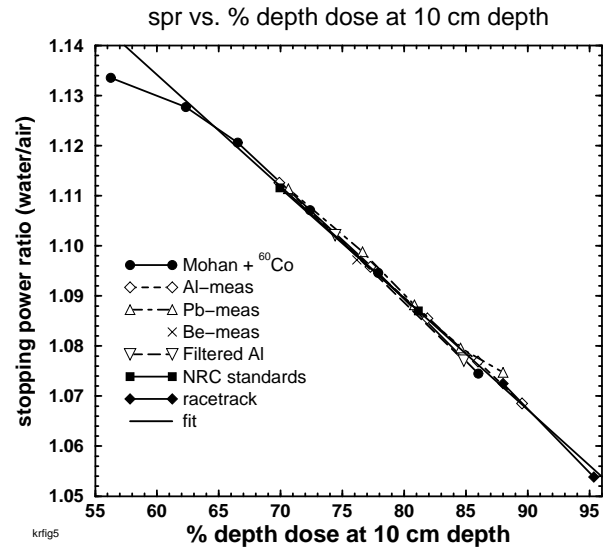


Figure 4: Water to air stopping-power ratios  $vs$   $\%dd(10)_x$  for the thick-target bremsstrahlung &  $^{60}\text{Co}$  spectra in figure 3. The straight line shown is the fit to the sprs of the bremsstrahlung beams given by eq.(16) with an rms deviation of 0.0013 and a maximum deviation of 0.003. From Kosunen and Rogers (1993).

for the photon component of the beam. This is shown in figure 4 and the line is given by:

$$\left(\frac{\bar{L}}{\rho}\right)_{\text{air}}^w = 1.2676 - 0.002224(\%dd(10)_x). \quad (16)$$

The problem with this relationship is that it applies only for photon beams with no electron contamination. In  $10 \times 10 \text{ cm}^2$  fields for beams above 10 MV, electron contamination affects the dose maximum and hence affects  $\%dd(10)$ , the measured % depth dose at 10 cm. Using 2 sets of measured data which demonstrated considerable variation from machine to machine, estimates have been made of the effects of electron contamination on  $\%dd(10)$  (see fig 5) and the linear correction needed is given by:

$$\%dd(10)_x = 1.2667(\%dd(10)) - 20.0 \quad [\text{for } \%dd(10) > 75\%]. \quad (17)$$

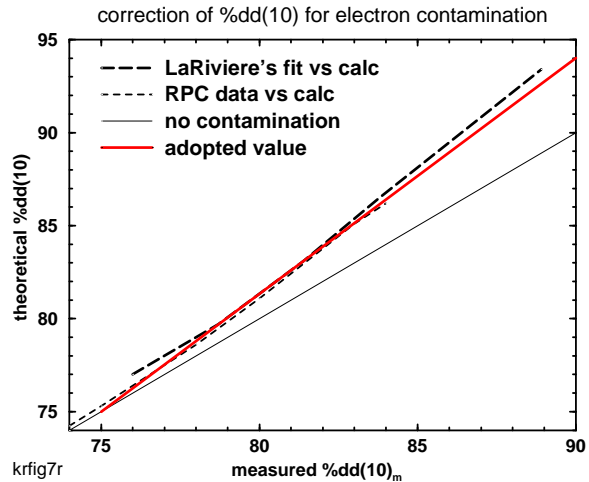
For  $\%dd(10) < 75\%$  one need make no adjustments,  $\%dd(10)_x = \%dd(10)$ . Especially for high energies this approach may lead to errors of up to 2% in the assigned value of  $\%dd(10)_x$  but as seen below, there is only a 0.2% error in  $k_Q$  values per 1% error in  $\%dd(10)_x$ .

Another approach for determining  $\%dd(10)_x$  has been investigated by Li and Rogers (1994). A 1 mm lead foil is inserted in the accelerator beam immediately below the accelerator head. This removes from the beam, all the electron contamination from the accelerator head (which is the source of the machine to machine variation) and adds a known amount of electron contamination to the beam which can be taken into account. For beams with  $\%dd(10)$  greater than 70%, the value of  $\%dd(10)_x$  in the *unfiltered* beam is given by:

$$\%dd(10)_x = [0.9439 + 0.000804(\%dd(10))] \%dd(10) - 0.15 \quad [\text{for } \%dd(10) > 70\%] \quad (18)$$

where  $\%dd(10)$  is measured in the *filtered* beam. For beams with  $\%dd(10) < 70\%$ , electron contamination plays no role and  $\%dd(10)_x = \%dd(10) - 0.15$  where  $\%dd(10)$  is measured in the filtered beam. The 0.15

Figure 5: Two estimates of the effects of electron contamination on %dd(10), based on measured data with considerable fluctuations. The adopted fit given by eq.(17) is shown as the darker solid line. Modified from Kosunen and Rogers (1993).



corrects for the slight beam hardening by the lead filter. However, for the low-energy beams it is more direct just to use  $\%dd(10)_x = \%dd(10)$  where  $\%dd(10)$  is measured in the unfiltered beam.

There is another aspect of measuring depth-dose curves with a cylindrical ion chamber which must be taken into account, *viz.* the change in the gradient correction factor (roughly a 1% effect). There is no gradient correction factor at dose maximum but at 10 cm depth, the correction varies with the beam quality and chamber radius ( $P_{\text{repl}}$  correction, see section 4.A.5). For measuring depth-dose curves, instead of using  $P_{\text{repl}}$ , this correction can be handled by treating a cylindrical or spherical ion chamber's point of measurement as being at  $0.75r$  upstream of the center of the chamber, where  $r$  is the radius of the chamber cavity (this is the point of measurement used by the IAEA Code of Practice and thus different from the TG-21 values of  $P_{\text{repl}}$ , as seen in figure 1). Note that for all other measurements in the TG-51 protocol, the point of measurement of cylindrical and spherical chambers is considered to be at the center. Although the issue of gradient corrections can be avoided by using diode detectors to measure the depth-dose curve, it is essential to ensure the diode is actually measuring dose since they can be very sensitive to low energy components in the beam which change with depth.

In summary, for photon beams it appears that the widely used  $\%dd(10)$  is an excellent beam quality specifier. Not only does it define a single value of the stopping-power ratio needed for photon beam dosimetry, it also maintains its sensitivity in high-energy photon beams and is relatively easy to measure. Some care must be taken to account for the changes in gradient effects at  $d_{\text{max}}$  and at 10 cm depth, and also to account for electron contamination for beams with  $\%dd(10)_x$  over 70%.

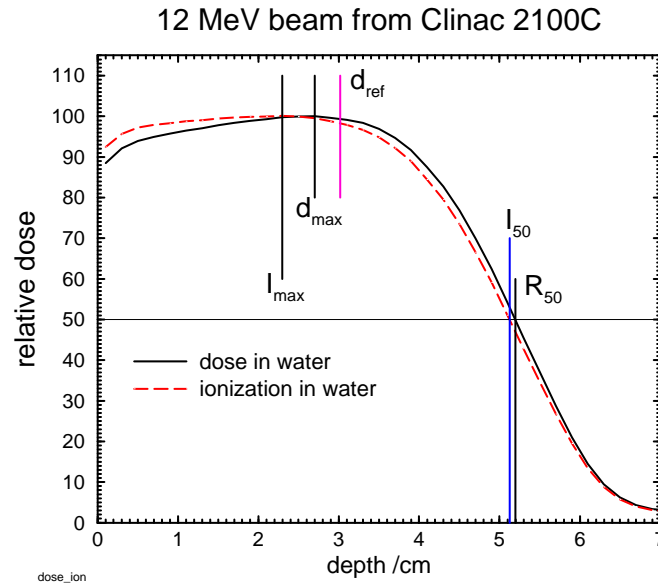
### 5.C. Specification of Electron Beam Quality

#### 5.C.1) Determination of $R_{50}$

Most protocols specify electron beam quality in terms of the mean energy of the beam at the patient surface,  $\bar{E}_0$ , which is determined by measuring  $R_{50}$ , the depth at which the dose in a broad beam falls to 50% of its maximum value. With TG-21 there was some discussion about using depth-dose or depth-ionization curves and  $\text{SSD} = 100 \text{ cm}$  *vs* correcting to parallel beam conditions (Wu *et al* 1984). Although the effects are not large, the correct procedure is to use the SSD corresponding to whatever use is being made of  $R_{50}$  and to use the value of  $R_{50}$  from the depth-dose curve. The problem is that to determine the depth-dose curve requires converting the ionization to dose using stopping-power ratios and these require knowledge of the  $R_{50}$ ! One way out of this loop is to determine  $I_{50}$  from the depth-ionization curve (using the effective point of measurement technique discussed in section 4.A.5) and then use the relationship developed by Ding *et al* (1995):

$$R_{50} = 1.029I_{50} - 0.063 \quad [\text{cm}] \quad (2.2 < I_{50} < 10.2 \text{ cm}). \quad (19)$$

Figure 6: Difference between a depth-ionization and depth-dose curve for a 12 MeV beam at SSD = 100 cm. The depths of dose and ionization maxima and 50% values are shown, as well as the reference depth,  $d_{\text{ref}} = 0.6R_{50} - 0.1$  (cm) (discussed in section 5.C.4). Based on data from Ding *et al* (1997).



This equation only applies to beams with initial energies between 5 and 25 MeV and is a more accurate version of the correction given in the IAEA Code of Practice(1987). Below 5 MeV no correction is needed and for higher-energy beams, fig.19 of the original paper should be used.

Another approach is to use  $I_{50}$  as a first approximation to  $R_{50}$  and to use a universal function developed by *et al.* (1996) which gives the water to air stopping-power ratio as a function of depth,  $z$ , and  $R_{50}$  with adequate accuracy for converting from depth-ionization to depth-dose curves, *viz.*:

$$\left(\frac{\bar{L}}{\rho}\right)_{\text{air}}^{\text{w}}(z, R_{50}) = \frac{a + b(\ln R_{50}) + c(\ln R_{50})^2 + d(z/R_{50})}{1 + e(\ln R_{50}) + f(\ln R_{50})^2 + g(\ln R_{50})^3 + h(z/R_{50})} \quad (20)$$

for  $z/R_{50}$  ranging between 0.02 and 1.2,  $R_{50}$  ranging between 1 and 19 cm and with:  $a = 1.0752$ ;  $b = -0.50867$ ;  $c = 0.088670$ ;  $d = -0.08402$ ;  $e = -0.42806$ ;  $f = 0.064627$ ;  $g = 0.003085$ ;  $h = -0.12460$ . Using these data allow direct conversion in terms of  $R_{50}$  without determining  $\bar{E}_o$  and tables of stopping-power ratios *vs* depth as a function of  $\bar{E}_o$ .

A third alternative is to determine the depth-dose curve using a good-quality diode detector which responds as a dose-detector (Rikner 1985; Khan *et al* 1991) and then determine  $R_{50}$ .

### 5.C.2) The mean energy at the phantom surface, $\bar{E}_o$

The TG-21 and IAEA protocols use the value of  $R_{50}$  (in cm) to determine the mean energy at the phantom surface,  $\bar{E}_o$  using:

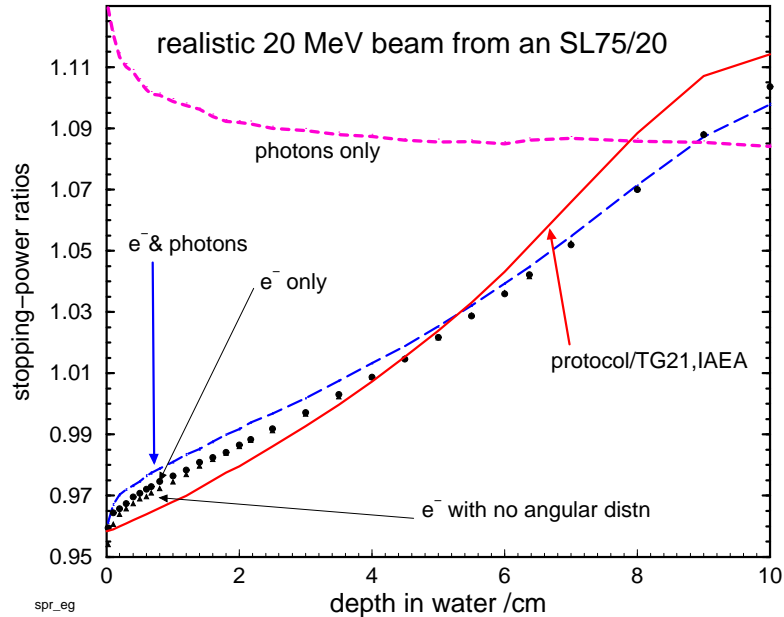
$$\bar{E}_o = 2.33R_{50} \quad [\text{MeV}]. \quad (21)$$

Rogers and Bielajew (1986) provided more accurate data for making this conversion which accounted for the finite SSD used in the measurement of  $R_{50}$  and more accurate Monte Carlo calculations than those that had been used to establish the 2.33 MeV/cm factor used in TG-21. These more accurate data were recommended by TG-25 on electron beam dosimetry (Khan *et al* 1991). However, all of the previous Monte Carlo calculations were done using mono-energetic electron beams. Ding *et al* (1996) have recently shown that  $\bar{E}_o$  and  $R_{50}$  do not correlate very well with the data of Rogers and Bielajew (1986) because scattered electrons in the beam affect  $\bar{E}_o$  but have little effect on  $R_{50}$ . On the other hand, the direct electrons in the beam, *i.e.* those that do not hit applicators or jaws *etc.*, do correlate well with the previous data.

### 5.C.3) Problems with stopping-power ratios using mono-energetic beams

In the TG-21 and IAEA protocols, the water to air stopping-power ratios needed for electron beam dosimetry are based on Monte Carlo calculations for mono-energetic electron beams. However, the energy and angular distributions of the real electron beams in the clinic have an effect on the stopping-power ratios (Andreo *et al* 1989; Andreo and Fransson 1989; Ding *et al* 1995). Figure 7 shows an example of the stopping-power ratios

Figure 7: Various Monte Carlo calculated water to air stopping-power ratios *vs* depth. The solid line represents the spr one would obtain following TG-21, the long dash, that from the complete simulation and the other curves include only some components of the beam. Based on data from Ding *et al* (1995).



calculated for a realistic beam simulation. The photon component of the beam and the electron spectrum have a pronounced effect on the stopping-power ratio although the angular distribution of the electrons has little effect. The size of the error made by assuming a mono-energetic beam varies with depth. The error can be up to 1.2% at  $d_{\max}$ . Thus, it is important to take into account the realistic nature of the beam when doing stopping-power ratio calculations. Ding *et al* (1995) gave a general procedure which uses the size of the bremsstrahlung tail to estimate the correction needed at  $d_{\max}$  for a stopping-power ratio determined assuming a mono-energetic beam.

### 5.C.4) Direct use of $R_{50}$ as beam quality specifier

Although the procedure developed by Ding *et al* (1995) takes into account the realistic nature of the beam, it is fairly complex to use, requiring several steps and, since  $d_{\max}$  varies considerably, a complete set of stopping-power ratios as a function of depth and incident mean energy  $\bar{E}_0$ . et al. (1996) found a much simpler solution, which by-passes much of the complexity of the previous methods and yet continues to take into account the realistic nature of the electron beams. The essence of the proposal is to change the reference depth for electron beam dosimetry from  $d_{\max}$  to  $d_{\text{ref}}$ :

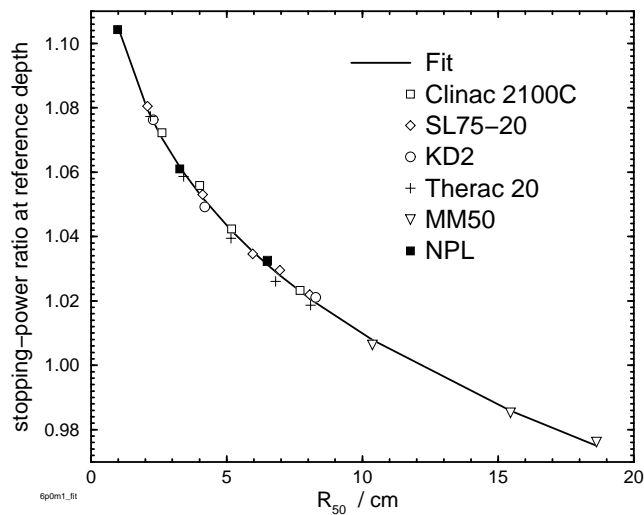
$$d_{\text{ref}} = 0.6R_{50} - 0.1 \quad [\text{cm}]. \tag{22}$$

For low-energy electron beams this depth corresponds closely to  $d_{\max}$  but for higher-energy beams it is past  $d_{\max}$ , but still usually well above a dose of 90% (see *e.g.* fig.6). The surprising feature about using this reference depth is that the water to air stopping-power ratio is given by:

$$\left(\frac{\bar{L}}{\rho}\right)_{\text{air}}^w(d_{\text{ref}}) = 1.2534 - 0.1487(R_{50})^{0.2144}, \tag{23}$$

for all clinical beams (the raw data are shown in figure 8). The rms deviation of the data about this fit is

Figure 8: Water to air stopping-power ratio at the reference depth  $d_{\text{ref}} = 0.6R_{50} - 0.1$  cm as a function of  $R_{50}$ . The fit is given by eq.(23). From et al. (1996).



0.16% with a maximum deviation of 0.26%. This equation replaces an entire page of stopping-power ratio data in the TG-21 protocol and is considerably more accurate since it applies to realistic beams. Also, it avoids the need to establish the mean energy at the surface of the phantom, a quantity which is not well defined by  $R_{50}$  (see section 5.C.2).

## 6. VALUES OF $k_Q$

### 6.A. Calculation of $k_Q$ Values

#### 6.A.1) An equation for $k_Q$

From eq.(1) for the dose to water in terms of the absorbed-dose calibration factor, one has:

$$N_{D,w}^Q = \frac{D_w^Q}{MP_{\text{ion}}^Q} \quad [\text{Gy/C}]. \quad (24)$$

Using eqs.(8), (9) and (13) for  $D_{\text{air}}$ ,  $D_w$  and  $M'$ , gives:

$$N_{D,w}^Q = \frac{K_h}{m_{\text{air}}} \left( \frac{W}{e} \right)_{\text{air}} \left( \frac{\bar{L}}{\rho} \right)_{\text{air}}^w P_{\text{wall}} P_{\text{fl}} P_{\text{gr}} P_{\text{cel}} \quad [\text{Gy/C}]. \quad (25)$$

Using eq.(2) to define  $k_Q$ , substituting eq.(25) at the two beam qualities, and assuming  $\left( \frac{W}{e} \right)_{\text{air}}$  is constant, one has:

$$k_Q = \frac{\left[ \left( \frac{\bar{L}}{\rho} \right)_{\text{air}}^w P_{\text{wall}} P_{\text{fl}} P_{\text{gr}} P_{\text{cel}} \right]_Q}{\left[ \left( \frac{\bar{L}}{\rho} \right)_{\text{air}}^w P_{\text{wall}} P_{\text{fl}} P_{\text{gr}} P_{\text{cel}} \right]_{60\text{Co}}}, \quad (26)$$

where the numerator and denominator are evaluated for the beam quality  $Q$  of interest, and the calibration beam quality,  $^{60}\text{Co}$ , respectively.

#### 6.A.2) Photon Beams

Calculation of  $k_Q$  for a given ion chamber in a photon beam is reasonably straight forward. One expects this formalism to be more accurate than a formalism starting from air-kerma standards since in this case,

only ratios of the same quantity at different beam qualities are needed rather than the value itself. For example, the effective value of the factor  $P_{\text{repl}}$  differs by at least 0.4% and up to 0.8% for the IAEA or TG-21 approaches (the solid and dashed lines in fig.(1)). However, the difference in the ratio of these values is never more than 0.4% when calculating  $k_Q$ . In effect, by using a primary standard for absorbed dose at  $^{60}\text{Co}$  energy, the uncertainty due to  $P_{\text{repl}}$  is reduced because this quantity is, in some senses, “included” in the primary standard.

In calculating  $k_Q$  with eq.(26), the values of  $(\bar{L}/\rho)_a^w$  as a function of  $\%dd(10)_x$  are calculated using eq.(16) for  $\%dd(10)_x \geq 62.2\%$ , and are interpolated linearly from there (1.1277) to the  $^{60}\text{Co}$  point at 56.3% (1.1335)(Kosunen and Rogers 1993). Since the variation in  $(\bar{L}/\rho)_a^w$  dominates the beam quality dependence, we expect the value of  $k_Q$  to be nearly linear with  $\%dd(10)_x$ , at least for beams with  $\%dd(10)_x > 62.2\%$ .

Ignoring issues about the accuracy of eq.(10), it can be used to calculate the  $P_{\text{wall}}$  term and if a thin-walled waterproofing sheath has been used, it can be ignored and  $\tau$  taken as 0.0 (see section 4.B.3). The physical data needed for this  $P_{\text{wall}}$  equation are taken from the IAEA Code of Practice (1987) since it uses stopping powers and mass energy absorption coefficients which are consistent with those used in the standards laboratories. These data are tabulated as a function of  $\text{TPR}_{10}^{20}$ . Since the variation in the overall  $P_{\text{wall}}$  factor is small, one can use a value of  $\text{TPR}_{10}^{20}$  from a fit to standard clinical beam data which gives (Rogers and Booth 1996):

$$\text{TPR}_{10}^{20} = -0.6391 + 0.029348 (\%dd(10)_x) - 0.00014498 (\%dd(10)_x)^2. \quad (27)$$

Note, this equation applies to  $\%dd(10)_x$  with electron contamination removed and it is not accurate enough to make the conversion from  $\%dd(10)_x$  to  $\text{TPR}_{10}^{20}$  in general: if it were, there would be no advantage in changing beam quality specifiers! The variation in  $P_{\text{wall}}$  factors for typical thin-walled ion chambers in photon beams is less than 1%.

The  $P_{\text{H}}$  term in eq.(26) is 1.00 in a photon beam (see section 4.A.5) and thus does not enter the calculation of  $k_Q$ .

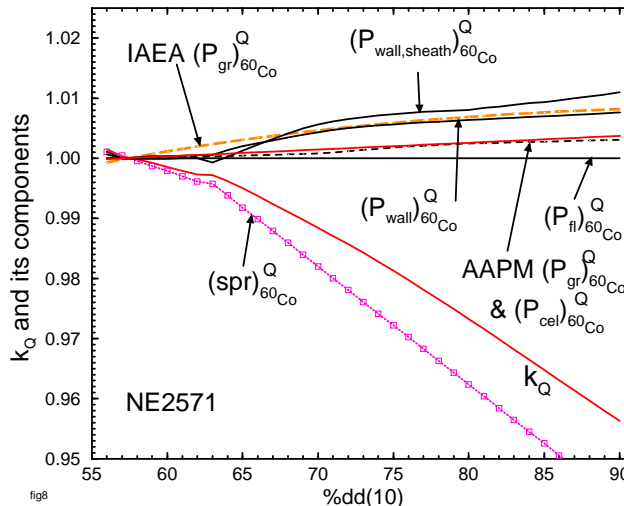
The  $P_{\text{gr}}$  term can be calculated using the data in fig.(1). Despite the large differences in the effective values used by the protocols, the difference in the ratio is quite small. Since the variation in the TG-21 value is close to the variation in the original data of Johansson *et al* (1977), and for continuity with past practice, it is easiest to use the value of  $P_{\text{gr}}$  from the TG-21 protocol, which is based on the work of Cunningham and Sontag (1980). This parameter is a function of beam quality and the diameter of the chamber’s gas cavity. For a Farmer-like chamber it only varies by about 0.4% as a function of beam quality.

The  $P_{\text{cel}}$  term, which only applies for chambers with an aluminum electrode, is calculated using eq.(12). For a 1 mm diameter aluminum electrode (the only size for which there are data), the effect on  $k_Q$  is an increase of less than 0.4%.

Figure 9 presents calculated  $k_Q$  values for an NE2571 cylindrical Farmer chamber with  $0.065 \text{ g/cm}^2$  walls, 6.3 mm cavity diameter and 1 mm diameter aluminum electrode. It also shows the contribution of each of the components in eq.(26), *e.g.*  $(P_{\text{wall}})_Q / (P_{\text{wall}})_{^{60}\text{Co}} = (P_{\text{wall}})_{^{60}\text{Co}}^Q$ . For comparison, two additional curves are shown. One is for the effective  $P_{\text{repl}}$  component from the IAEA Code of Practice and the second shows the effect on  $P_{\text{wall}}$  of considering a 1 mm thick PMMA waterproofing sheath as in eq.(10). This figure indicates, most importantly, that the stopping-power ratio dominates the change with beam quality in  $k_Q$  and hence the calibration factor  $N_{\text{D,w}}^Q$ . Secondly, the effect of ignoring the sheath is about 0.3% at high energies, a value which is consistent with the experimental data (see section 4.A.4). Finally, the uncertainty in the correct value of  $P_{\text{repl}}$  continues to be the major uncertainty in the calculation of  $k_Q$ .

For cylindrical ion chambers with walls thinner than  $0.25 \text{ g/cm}^2$ , there is a “universal” curve for  $k_Q$  which agrees with the individual calculations within  $\pm 1\%$  and for Farmer-like chambers this is further improved to an accuracy of  $\pm 0.7\%$  (Rogers 1992c). Figure 9 shows that this is possible because the major determinant of  $k_Q$  is the stopping-power ratio and this is independent of the ion chamber. The next largest factor is the  $P_{\text{wall}}$  factor and this is mostly determined by the wall material. Thus, calculated  $k_Q$  values for Farmer-like ion chambers of a particular wall material are all very nearly the same. Figure 10 shows such a set of  $k_Q$  values which apply within a few tenths of a percent for all commercial ion chambers for which calculations

Figure 9: Calculated values of  $k_Q$  and its components for an NE2571 Farmer-like ion chamber with  $0.065 \text{ g/cm}^2$  graphite walls, inner diameter of 6.3 mm and an aluminum electrode with 1 mm diameter. The TG-21  $P_{\text{repl}} = P_{\text{gr}}$  component (short dash) and the  $P_{\text{cel}}$  component defined here (solid line) are almost the same. Also shown for comparison are the  $P_{\text{wall}}$  component including consideration of a 1 mm PMMA waterproofing sheath and the effective  $P_{\text{repl}}$  component based on the IAEA Code of Practice.



have been done (although there is slightly more spread than in the original paper (Rogers 1992c) since the  $P_{\text{cel}}$  correction has been included here).

Figure 10: Calculated values of  $k_Q$  for cylindrical Farmer-like ion chambers with the walls shown. These values apply within a few tenths of a percent for all chambers studied (Rogers (1992d), updated).

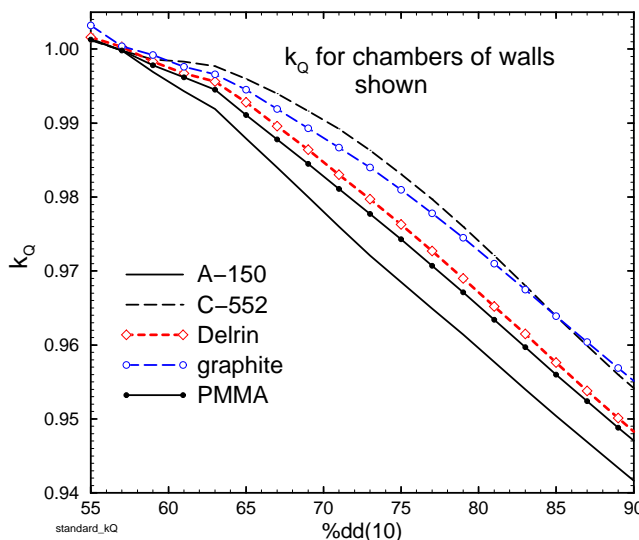
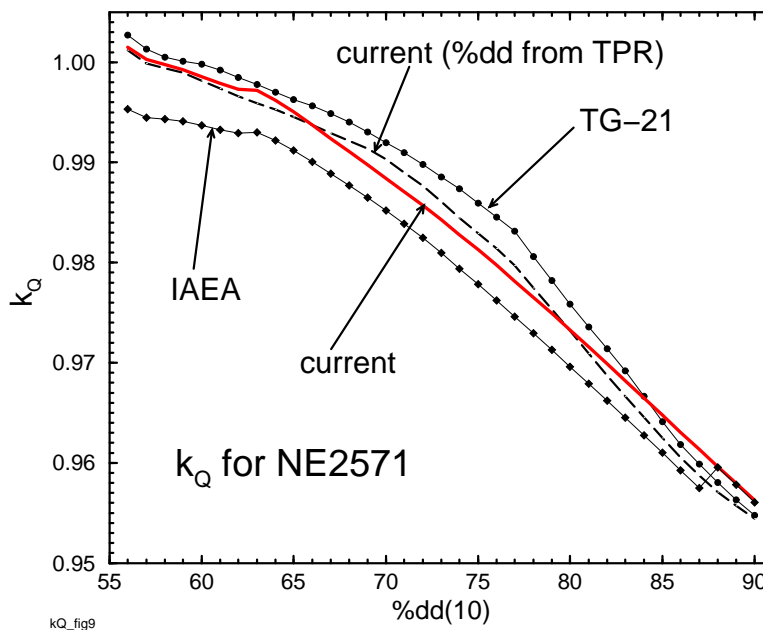


Figure 11 compares the present results to results that would be obtained using previous protocols and the data in them. The change from TG-21 values is not large, and mostly accounted for by the change in the underlying stopping powers being used now. However, the difference would be slightly larger if there were no aluminum electrode since this was not considered in TG-21 and it affects this chamber. Also, part of the difference comes from the uncertainty introduced by interpolating the previous AAPM data which was presented as a function of  $\text{TPR}_{10}^{20}$  whereas here  $\%dd(10)_x$  is used. The IAEA values differ considerably because of how they treated  $^{60}\text{Co}$  beams as a special case. Note also that the IAEA’s correction for the central electrode only “kicks-in” for high-energy beams ( $\%dd(10)_x > 87\%$ ), but when it does, the value it uses is close to that used here (although the definitions differ so that  $P_{\text{cel}}(\text{IAEA}) = P_{\text{cel}}(Q)/P_{\text{cel}}(^{60}\text{Co})$ ).

PROT, a program for calculating  $k_Q$  for arbitrary chambers has been written (Rogers and Booth 1996). It is based on the program described earlier (Rogers 1992c) but updated to take into account the changes described above. It will be made available via the WWW at the address given at the beginning of this references. There are also several very extensive sets of calculated  $k_Q$  values available in the literature (Andreo 1992; Rogers 1992c) but these are given as a function of  $\text{TPR}_{10}^{20}$  and do not include the  $P_{\text{cel}}$  correction used here.

Figure 11: Values of  $k_Q$  for NE2571 cylindrical chamber with  $0.065 \text{ g/cm}^2$  graphite walls, cavity of 6.3 mm and 1 mm diameter aluminum electrode. Results use eq.(27). Part of the difference for TG-21 is that previous data are tabulated *vs*  $\text{TPR}_{10}^{20}$  and require a conversion from  $\%dd(10)_x$  to  $\text{TPR}_{10}^{20}$ . The current results are also shown using this approach to show the variations introduced.



### 6.A.3) Electron Beams

Calculation of  $k_Q$  for electron beams is considerably more complex than for photon beams since the quantities in the numerator and denominator of eq.(26) are different, not just the same quantities at slightly different beam qualities as in the photon beam case. Also, for electron beams one must handle plane-parallel chambers since these are recommended for use in low-energy beams.

For cylindrical chambers, the denominator of eq.(26) is calculated in the same manner as in section 6.A.2). For plane-parallel chambers the denominator evaluated in  $^{60}\text{Co}$  beams requires some new considerations. The stopping-power ratio is the same as in the cylindrical chamber case. The  $P_{\text{repl}}$  factor for plane-parallel chambers is unity (see section 4.A.5). The  $P_{\text{cel}}$  factor is unity since there are no central electrodes. The  $P_{\text{wall}}$  factor is not covered by eq.(10) which only applies to chambers where the wall uniformly surrounds the cavity. For plane-parallel chambers, the front wall is often much thinner than the rest of the chamber and of a different material. Also, any insulator material immediately behind the cavity may have a dramatic effect on the response (up to 5%) and  $P_{\text{wall}}$  must take this into account (Rogers 1992a; Almond *et al* 1994). In the TG-39 report on electron beam dosimetry with plane-parallel chambers (which, for consistency with TG-21 did not use the ICRU Report 37 stopping powers being used here), values of  $P_{\text{wall}}$  in a  $^{60}\text{Co}$  beam were provided for the case in which the phantom material matched the major component of the chamber (graphite for an NACP chamber, PMMA for a Markus chamber, *etc*). For the present purposes, we need the value of  $P_{\text{wall}}$  in a water phantom, which also implies there may be a waterproofing cap on the plane-parallel chamber. Using the same methods as previously, I have done a further series of Monte Carlo calculations and derived the necessary values for various commercial plane-parallel chambers (see table 3). Note that these values are for  $^{60}\text{Co}$  only, and since values of  $P_{\text{wall}}$  are not usually available for other photon beam qualities, plane-parallel chambers are not suitable for absorbed-dose measurements in photon beams until there are measured values of  $P_{\text{wall}}$ , or preferably  $k_Q$ , available.

With  $P_{\text{wall}}$  values available, all the factors in the denominator of eq.(26) are known (the denominator is just  $N_{\text{D,w}}^{60\text{Co}}/N_{\text{gas}}$  in TG-21 terminology). These values of the denominator are calculated and have a relatively large systematic uncertainty. Once it is decided how to waterproof each of these chambers properly, something some of the manufacturers have already done, it would be preferable to have these values measured.

For the numerator in eq.(26) for  $k_Q$  for electron beams, the stopping-power ratio term is given by eq.(23) since these values are all for the reference depth,  $0.6R_{50} - 0.1 \text{ cm}$ . I will take the  $P_{\text{wall}}$  term to be unity, with

Table 3:  $P_{\text{wall}}$  correction factor for plane-parallel chambers in a phantom of the major material of the chamber or water, irradiated by  $^{60}\text{Co}$  beams (Rogers tted). Uncertainties shown are statistical (68% confidence) and there is an inherent 1% systematic uncertainty. For the in-water case, it is assumed a 1 mm slab of the major material of the chamber is used for waterproofing.

Chamber (major material)	$P_{\text{wall}}$ in $^{60}\text{Co}$ beam	
	in homogeneous phantom	in water with 1 mm sheath
Attix Chamber (RMISW)	1.012(3)	1.023(3)
Capintec PS033 (polystyrene)	0.948(1)	0.974(3)
Exradin P11 (polystyrene)	0.991(5)	1.021(3)
Holt (polystyrene)	0.992(2)	0.994(4) <sup>a)</sup>
Markus (PMMA)	0.992(2)	0.998(2)
NACP (graphite)	1.018(2)	1.018(2) <sup>b)</sup>
PTB/Roos (PMMA)	0.995(2)	1.002(2)

<sup>a)</sup> 4 mm polystyrene front face in place over entire sheet.

<sup>b)</sup> Thin mylar sheet over front graphite face for waterproofing.

the caveat expressed in section 4.A.4), that for plane-parallel chambers, there may be a need to include a factor varying between 1.0 and 1.02, depending on the energy and material of the back wall of the chamber. The  $P_{\text{cel}}$  factor for cylindrical chambers with 1 mm aluminum electrodes is 1.000 or 0.998 as given in table 2.

The remaining correction in the numerator of eq.(26) for electron  $k_{\text{Q}}$  values is  $P_{\text{repl}} = P_{\text{fl}}P_{\text{gr}}$ . For plane-parallel chambers there is no problem with the gradient correction,  $P_{\text{gr}}$ , which is taken to be 1.00 in electron beams because the point of measurement is taken at the front of the air cavity. For well-guarded plane-parallel chambers,  $P_{\text{fl}}$  is also taken as unity, but this is not the case for the Markus and Capintec chambers (section 4.A.5), and their tabulated  $P_{\text{fl}}$  values are given here by the expressions in fig 2 using the same techniques as described below for estimating the mean energy,  $\bar{E}_z$ , at  $d_{\text{ref}}$ . Also, most data for these chambers have been measured at  $d_{\text{max}}$  and there are likely variations at other depths.

For cylindrical chambers, handling these correction factors is more complex. Values of  $P_{\text{fl}}$  for cylindrical chambers are a function of chamber radius and the mean energy at the point measurement and these values are given in TG-21 (see section 4.A.5). Despite the fact that these values are only known for  $d_{\text{max}}$  and we now need them at  $d_{\text{ref}}$ , we will assume that the values in TG-21 still apply (and encourage some measurements to establish the correct value). For low-energy beams these values apply because  $d_{\text{ref}}$  is still at  $d_{\text{max}}$ . At higher energies, the correction becomes less important and thus the approximation being used is probably acceptable. We still need to evaluate  $\bar{E}_z$ , the mean energy at the point of measurement. Traditionally this is given by the Harder relationship:

$$\bar{E}_z = \bar{E}_o(1 - z/R_p), \quad (28)$$

where  $\bar{E}_o$  is the mean energy at the surface and  $R_p$  is the practical range (ICRU 1984a). This parameterization unfortunately breaks with the proposed beam quality specification in terms of  $R_{50}$ . However, it is possible to recast the data on  $P_{\text{fl}}$  so that the value of  $P_{\text{fl}}$  at  $d_{\text{ref}}$  is given as a function of  $R_{50}$  and the cavity radius. An approximate value of  $\bar{E}_o$  is given by  $2.33R_{50}$  and fitting data for  $R_p$  and  $R_{50}$  from Ding and Rogers (1995), one can write:

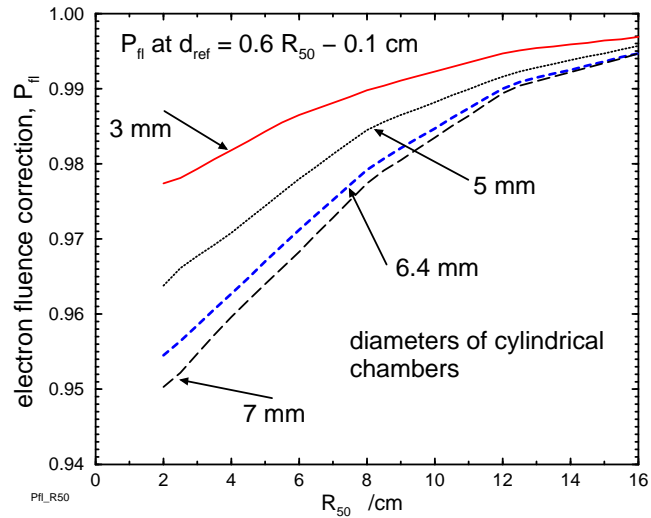
$$R_p = 1.271R_{50} - 0.23 \quad [\text{cm}]. \quad (29)$$

Putting these relationships together leads to the data in fig 12. Note that because the reference depth,  $d_{\text{ref}}$ , is deeper than  $d_{\text{max}}$  for high energies, the  $P_{\text{fl}}$  correction is significant, even at high energies (it is about 0.98 for a Farmer-like chamber at  $d_{\text{ref}}$  in a 20 MeV beam).

The remaining problem in the evaluation of eq.(26) for electron beams is that of  $P_{\text{gr}}$  at  $d_{\text{ref}}$ . For low-energy beams where  $d_{\text{ref}}$  is at  $d_{\text{max}}$ ,  $P_{\text{gr}} = 1.0$ , and the same is true for plane-parallel chambers at all energies. However, in general this correction depends on the specific depth-dose curve being measured and hence cannot be tabulated. Because of this fact, for electron beams one has:

$$k_{\text{Q}} = k_{R_{50}}k_{\text{gr}}, \quad (30)$$

Figure 12: Values of  $P_{fl}$  at a depth of  $d_{ref}$  vs  $R_{50}$  for cylindrical ion chambers. Based on data in TG-21 from Johansson *et al* (1977) and using the techniques from Rogers and Booth (1996) to relate the various parameters.



where:

$$k_{R_{50}} = \frac{\left[ \left( \frac{\bar{L}}{\rho} \right)_{air}^w P_{wall} P_{fl} P_{cel} \right]_{R_{50}}}{\left[ \left( \frac{\bar{L}}{\rho} \right)_{air}^w P_{wall} P_{fl} P_{gr} P_{cel} \right]_{^{60}Co}}, \quad (31)$$

and:

$$k_{gr} = 1 - 0.5r_{cav}G/100, \quad [\text{for cylindrical chambers}] \quad (32)$$

$$= 1.0 \quad [\text{for plane-parallel chambers or at } d_{max}] \quad (33)$$

where<sup>1</sup>  $r_{cav}$  is the radius of the chamber's cavity in mm and  $G$  is the dose gradient at  $d_{ref}$  (% change in dose per mm, which can be taken as the percentage change in the ion chamber reading going from  $d_{ref}$  to  $d_{ref} + 0.5r_{cav}$ <sup>2</sup> divided by  $0.5r_{cav}$ ). *et al.* (1996) have shown  $G$  is typically 1% or less, and hence  $k_{gr}$  is within 1.6% of unity for a Farmer-like chamber. This  $k_{gr}$  correction is equivalent to using the point of measurement for cylindrical chambers recommended by the IAEA Code of Practice (1987) and the AAPM's TG-25 (Khan *et al* 1991).

With all of the above in place, it is possible to present curves of  $k_Q$  values for plane-parallel chambers (fig.13) and curves of  $k_{R_{50}}$  for cylindrical chambers (fig.14). Unfortunately, these curves cannot be generalized as easily as in the case for photon beams. For the NACP, Exradin, Attix, Holt and PTB/ Roos plane-parallel chambers, the differences between the curves are completely determined by the value of  $P_{wall}$  for the chamber in a water phantom irradiated by a <sup>60</sup>Co beam although recall that possible variations with  $P_{wall}$  in the electron beams have not been included. For the Markus and Capintec chambers, the effect of  $P_{fl}$  also plays a significant role, especially for the lower energies. For the cylindrical chambers, several factors are at work causing the differences seen in fig. 14. For one thing,  $P_{fl}$  is strongly affected by the radius of the cavity (see fig. 12). Also, the values of  $P_{wall}$  in the <sup>60</sup>Co beam vary by 2.8%, or 1% going from the thin to thick walls for the chambers with air-equivalent plastic C552 walls. For the NE2571 chamber, the central electrode effect increases  $k_{R_{50}}$  by 0.7% for low energy beams and 0.5% for beams above 13 MeV. The shoulder in this curve is at the transition point in the  $P_{cel}$  correction.

Another approach which would make the  $k_Q$  curves more similar, is to define  $k_Q$  for electron beams with respect to an absorbed-dose calibration factor in a reference electron beam (presumably at high energies since primary standards can be more easily developed there). In this case, instead of using a <sup>60</sup>Co calibration factor in eq.(3), one uses the electron beam calibration factor:

$$D_w^Q = MP_{ion} k_Q^e N_{D,w}^e \quad [\text{Gy}]. \quad (34)$$

<sup>1</sup>Eq.(32) was published as  $k_{gr} = 1 + 0.5r_{cav}G/100$ .

<sup>2</sup>This was published as  $d_{ref} - 0.5r_{cav}$ .

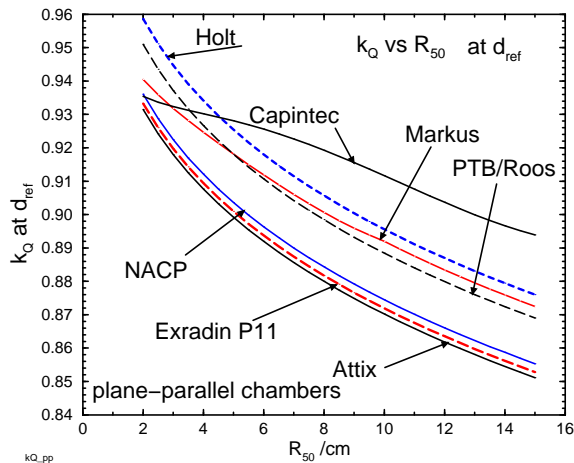


Figure 13: Calculated values of  $k_Q$  for plane-parallel chambers used in a water phantom at  $d_{ref}$ . Values apply for Chambers are assumed waterproofed as described in table 3.

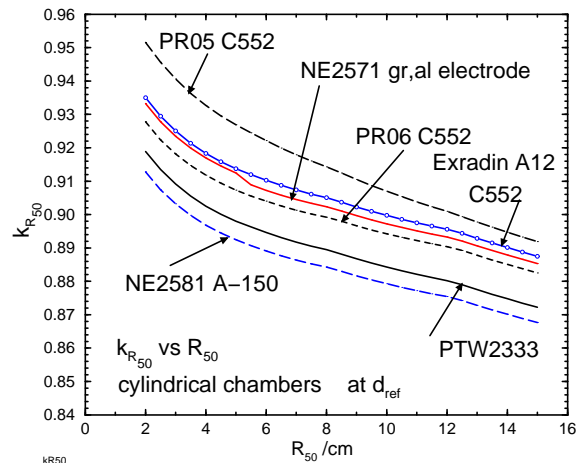


Figure 14: Calculated values of  $k_{R_{50}}$  for commonly used cylindrical ion-chambers. Values apply for measurements at  $d_{ref}$  in a water phantom.

The advantage of this equation is that, except for differences in  $P_{fl}$ , the  $k_Q$  or  $k_{R_{50}}$  curves will be identical for different detectors. To handle this in a protocol based on  $^{60}\text{Co}$  absorbed-dose calibration factors requires an extra piece of data, *viz.*  $k_{el}$ , the ratio of  $N_{D,w}^e$  to  $N_{D,w}^{60Co}$ . In this case, in electron beams one has:

$$D_w^Q = MP_{ion} k_Q^e k_{el} N_{D,w}^{60Co} \quad (35)$$

Note that the factor  $k_{el}$  is just the standard  $k_Q$  for the beam quality chosen for the reference electron beam.

## 6.B. Measurement of $k_Q$ Values

As mentioned above (section 3.), the ideal situation is to have  $k_Q$  values measured using primary standards of absorbed dose for all beam qualities of interest for all chambers which are used in the clinic. This is impossible, especially since there are no primary standards in place for electron beams in North America. However, on the photon side, there have been a variety of measurements reported (Shortt *et al* 1993; Boutillon *et al* 1994; Ross *et al* 1994; Guerra *et al* 1995; Vatnitsky *et al* 1995), not all of which use primary standards, and not many of which have sorted out the issues of beam quality specification (see section 5.B.). At the present time there is a major project underway at NRC which will use primary standards at several photon beam qualities to calibrate 3 each of 6 widely used Farmer-like cylindrical chambers and specify the beam quality in a wide variety of manners to elucidate the best manner of doing this. Seuntjens *et al* (1996) are reporting on this work at this years AAPM meeting. The already published data has shown clearly that the calculated values of  $k_Q$  are accurate within about 1% but there are demonstrable problems with beam quality specification using  $\text{TPR}_{10}^{20}$  which can lead to 0.5% problems or more. Furthermore, there are known problems with the calculated  $P_{wall}$  factors at about the 0.5% level. Within the next year, there should be a large amount of reliable data available for photon beams, which will both allow measured data to be used for many common detectors, or allow calculations to be done with considerable accuracy.

For electron beams, the promise of directly measured  $k_Q$  factors is further in the future. In the meantime, it would be very useful if further investigations were done on fluence and gradient corrections at the new reference depth,  $d_{ref}$  and on the measurement of water phantom  $P_{wall}$  factors for plane-parallel chambers in  $^{60}\text{Co}$  beams.

## 7. SUMMARY

To summarize, there have been a large number of improvements in the understanding of radiation dosimetry in the 15 years since TG-21 was developed. The most important feature is that there are now primary standards of absorbed dose to water which can be used in accelerator photon beams and hence the ability to make clinical measurements at the 1% level under reference conditions is, in principle, here. The new TG-51 protocol will incorporate the use of these new standards and a variety of new approaches which should make clinical dosimetry both simpler and more accurate. Since the assigned clinical doses will not usually be very different from those assigned using TG-21, the transition should not be as difficult as it was when adopting TG-21. The ADCL's and national standards laboratories are already working on procedures for providing the absorbed-dose calibration factors needed instead of air-kerma calibration factors. Since the overall TG-51 protocol should be much simpler and easier to understand than the TG-21 protocol, it is hoped that people will adopt it quickly and with little hassle.

This document does not present the TG-51 protocol, and many details which are dealt with in the protocol have been left out. However, the current draft of the protocol is prescriptive in nature, with the intention of making it easy to use. This chapter is actually much longer than the current draft of the protocol itself.

## 8. ACKNOWLEDGMENTS

I have benefited from many thought provoking discussions with my colleagues on TG-51, *viz.* Peter Almond, Peter Biggs, Bert Coursey, Will Hanson, Saiful Huq, Ravi Nath, and early on, Herb Attix. I would also like to thank my colleagues at NRC (Carl Ross, Jan Seuntjens, Charlie Ma, Ken Shortt, Norman Klassen and Alex Bielajew) for much work in this area plus Alan Nahum, David Burns, Pedro Andreo and Klaus Hohlfeld for stimulating discussions over the years.

## 9. REFERENCES

e-mail: dave@irs.phy.nrc.ca

WWW: [http://www.irs.inms.nrc.ca/inms/irs/papers/irs\\_www/irs\\_www.html](http://www.irs.inms.nrc.ca/inms/irs/papers/irs_www/irs_www.html)

- AAPM TG-21 (1983). A protocol for the determination of absorbed dose from high-energy photon and electron beams. *Med. Phys.* 10: 741 – 771.
- AAPM TG-21 (1984). Erratum: A protocol for the determination of absorbed dose from high-energy photon and electron beams. *Med. Phys.* 11: 213.
- Almond, P. R., Attix, F. H., Goetsch, S., Humphries, L. J., Kubo, H., Nath, R., and Rogers, D. W. O. (1994). The calibration and use of plane-parallel ionization chambers for dosimetry of electron beams: An extension of the 1983 AAPM protocol, Report of AAPM Radiation Therapy Committee Task Group 39. *Med. Phys.* 21: 1251 – 1260.
- Andreo, P. (1992). Absorbed dose beam quality factors for the dosimetry of high-energy photon beams. *Phys. Med. Biol.* 37: 2189 – 2211.
- Andreo, P. (1993). The status of high-energy photon and electron beam dosimetry five years after the implementation of the IAEA code of practice in the Nordic countries. *Acta Oncologica* 32: 483 – 500.
- Andreo, P. and Brahme, A. (1986). Stopping-power data for high-energy photon beams. *Phys. Med. Biol.* 31: 839 – 858.
-

- Andreo, P., Brahme, A., Nahum, A. E., and Mattsson, O. (1989). Influence of energy and angular spread on stopping-power ratios for electron beams. *Phys. Med. Biol.* 34: 751 – 768.
- Andreo, P. and Fransson, A. (1989). Stopping-power ratios and their uncertainties for clinical electron beam dosimetry. *Phys. Med. Biol.* 34: 1847 – 1861.
- Attix, F. H. (1986). *Introduction to Radiological Physics and Radiation Dosimetry*. New York: Wiley.
- Berger, M. J. and Seltzer, S. M. (1983). Stopping power and ranges of electrons and positrons. NBS Report NBSIR 82-2550-A (second edition).
- Bielajew, A. F. and Rogers, D. W. O. (1992). Implications of new correction factors on primary air kerma standards in  $^{60}\text{Co}$  beams. *Phys. Med. Biol.* 37: 1283 – 1291.
- Boag, J. W. (1987). Ionization Chambers. In K. R. Kase, B. E. Bjärngard, and F. H. Attix (Eds.), *The Dosimetry of Ionizing Radiation, Vol II*, pp. 169 – 243. Academic Press.
- Boutillon, M., Coursey, B. M., Hohlfeld, K., Owen, B., and Rogers, D. W. O. (1994). Comparison of primary water absorbed dose standards. IAEA-SM-330/48, in Proceedings of Symposium on Measurement Assurance in Dosimetry, (IAEA, Vienna): 95 – 111.
- Boutillon, M. and Perroche-Roux, A. M. (1987). Re-evaluation of the W value for electrons in dry air. *Phys. Med. Biol.* 32: 213 – 219.
- Cunningham, J. R. and Schulz, R. J. (1984). On the selection of stopping-power and mass-energy absorption coefficient ratios for high energy x-ray dosimetry. *Med. Phys.* 11: 618 – 623.
- Cunningham, J. R. and Sontag, M. R. (1980). Displacement Corrections Used in Absorbed Dose Determinations. *Med. Phys.* 7: 672 – 676.
- Ding, G. X. and Rogers, D. W. O. (1995). Energy spectra, angular spread, and dose distributions of electron beams from various accelerators used in radiotherapy. National Research Council of Canada Report PIRS-0439:  
(see <http://www.irs.inms.nrc.ca/inms/irs/papers/PIRS439/pirs439.html>).
- Ding, G. X., Rogers, D. W. O., Cygler, J., and Mackie, T. R. (1997). . *Med. Phys.*
- Ding, G. X., Rogers, D. W. O., and Mackie, T. R. (1995). Calculation of stopping-power ratios using realistic clinical electron beams. *Med. Phys.* 22: 489 – 501.
- Ding, G. X., Rogers, D. W. O., and Mackie, T. R. (1996). . *Med. Phys.* 23: 361 – 376.
- Domen, S. R. (1994). A sealed water calorimeter for measuring absorbed dose. *J of Res of NIST* 99: 121 – 141.
- Domen, S. R. and Lamperti, P. J. (1974). A Heat-Loss-Compensated Calorimeter: Theory, Design and Performance. *J. of Res. of NBS* 78A: 595 – 610.
- et al., B. (1996). . *Med. Phys.*
- Feist, H. (1982). Determination of the absorbed dose to water for high-energy photons and electrons by total absorption of electrons in ferrous sulphate solution. *Phys. Med. Biol.* 27: 1435 – 1447.
- Gillin, M. T., Kline, R. W., Niroomand-Rad, A., and Grimm, D. F. (1985). The effect of thickness of the waterproofing sheath on the calibration of photon and electron beams. *Med. Phys.* 12: 234 – 236.
- Guerra, A. S., Laitano, R. F., and Pimpinella, M. (1995). Experimental determination of the beam quality dependence factors,  $k_Q$ , for ionization chambers used in photon and electron dosimetry. *Phys. Med. Biol.* 40: 1177 – 1190.
- Hanson, W. F. and Tinoco, J. A. D. (1985). Effects of plastic protective caps on the calibration of therapy beams in water. *Med. Phys.* 12: 243 – 248.
- Hohlfeld, K. (1988). The standard DIN 6800: Procedures for absorbed dose determination in radiology by the ionization method. in Proc. of 1987 Symposium on Dosimetry in Radiotherapy (IAEA, Vienna) Vol 1: 13 – 24.
- Hunt, M. A., Kutcher, G. J., and Buffa, A. (1988). Electron backscatter correction for parallel-plate chambers. *Med. Phys.* 15: 96 – 103.
-

- IAEA (1987). *Absorbed Dose Determination in Photon and Electron Beams; An International Code of Practice*, Volume 277 of *Technical Report Series*. Vienna: IAEA.
- ICRU (1984a). Radiation Dosimetry: Electron beams with energies between 1 and 50 MeV. ICRU Report 35, ICRU, Washington D.C.
- ICRU (1984b). Stopping powers for electrons and positrons. ICRU Report 37, ICRU, Bethesda, MD.
- ICRU (1990). ICRU Report Committee Activities. in ICRU News(ICRU, Bethesda MD), June: 20.
- Johansson, K. A., Mattsson, L. O., Lindborg, L., and Svensson, H. (1977). Absorbed-dose determination with ionization chambers in electron and photon beams having energies between 1 and 50 MeV. IAEA Symposium Proceedings, (Vienna) IAEA-SM-222/35: 243 – 270.
- Khan, F. M. (1991). Replacement correction ( $P_{\text{repl}}$ ) for ion chamber dosimetry. *Med. Phys.* 18: 1244 – 1246.
- Khan, F. M., Doppke, K. P., Hogstrom, K. R., Kutcher, G. J., Nath, R., Prasad, S. C., Purdy, J. A., Rozenfeld, M., and Werner, B. L. (1991). Clinical electron-beam dosimetry: Report of AAPM Radiation Therapy Committee Task Group 25. *Med. Phys.* 18: 73 – 109.
- Klevenhagen, S. C. (1991). Implications of electron backscatter for electron dosimetry. *Phys. Med. Biol.* 36: 1013 – 1018.
- Kosunen, A. and Rogers, D. W. O. (1993). Beam Quality Specification for Photon Beam Dosimetry. *Med. Phys.* 20: 1181 – 1188.
- LaRiviere, P. D. (1989). The quality of high-energy X-ray beams. *Br. J. of Radiology* 62: 473 – 481.
- Lempert, G. D., Nath, R., and Schulz, R. J. (1983). Fraction of ionization from electrons arising in the wall of an ionization chamber. *Med. Phys.* 10: 1 – 3.
- Li, X. A. and Rogers, D. W. O. (1994). Reducing Electron Contamination for Photon-Beam-Quality Specification. *Med. Phys.* 21: 791 – 798.
- Ma, C.-M. and Nahum, A. E. (1993). Effect of size and composition of central electrode on the response of cylindrical ionisation chambers in high-energy photon and electron beams. *Phys. Med. Biol.* 38: 267 – 290.
- Ma, C.-M. and Rogers, D. W. O. (1995). Monte Carlo calculated wall correction factors for plane-parallel chambers in high-energy electron beams. *Med. Phys.* (abstract) 22: 672.
- Mattsson, L. O., Johansson, K. A., and Svensson, H. (1981). Calibration and use of plane-parallel ionization chambers for the determination of absorbed dose in electron beams. *Acta Radiol. Ther. Phys. Biol.* 20: 385 – 399.
- Mijnheer, B. J. and Williams, J. R. (1985). Comments on dry air or humid air values for physical parameters used in the AAPM protocol for photon and electron dosimetry. *Med. Phys.* 12: 656 – 658.
- NACP (1980). Procedures in external beam radiation therapy dosimetry with photon and electron beams with maximum energies between 1 and 50 MeV. *Acta Radiol. Oncol.* 19: 55 – 79.
- Nahum, A. E. (1978). Water/Air Stopping-Power Ratios for Megavoltage Photon and Electron Beams. *Phys. Med. Biol.* 23: 24 – 38.
- Nahum, A. E. (1988). Extension of the Spencer-Attix Cavity Theory to the 3-Media Situation for Electron Beams. in “Dosimetry in Radiotherapy”, (IAEA, Vienna) Vol 1: 87 – 115.
- Nahum, A. E. (1994). Perturbation Effects in Dosimetry. Technical Report ICR-PHYS-1/94, Joint Dept of Physics, The Royal Marsden Hospital, Sutton, Surrey, SM2 5PT, UK.
- Nath, R. and Huq, M. S. (1995). Advances in Radiation Dosimetry. In A. R. Smith (Ed.), *Radiation Therapy Physics*, pp. 401 – 448. Springer-Verlag.
- Pruitt, J. S., Domen, S. R., and Loevinger, R. (1981). The Graphite Calorimeter as a Standard of Absorbed Dose for  $^{60}\text{Co}$  Gamma Radiation. *J of Res. of NBS* 86: 495 – 502.
- Rikner, G. (1985). Characteristics of a p-Si detector in high energy electron fields. *Acta Rad. Oncol.* 24: 71 – 74.
-

- Rogers, D. W. O. (1992a). Calibration of Parallel-Plate Ion Chambers: Resolution of Several Problems by Using Monte Carlo Calculations. *Med. Phys.* 19: 889 – 899.
- Rogers, D. W. O. (1992b). New Dosimetry Standards. In J. Purdy (Ed.), *Advances in Radiation Oncology Physics, Medical Physics Monograph 19*, pp. 90 – 110. AAPM, New York.
- Rogers, D. W. O. (1992c). The advantages of absorbed-dose calibration factors. *Med. Phys.* 19: 1227 – 1239.
- Rogers, D. W. O. (1992d). Fundamentals of High Energy X-ray and Electron Dosimetry Protocols. In J. Purdy (Ed.), *Advances in Radiation Oncology Physics, Medical Physics Monograph 19*, pp. 181 – 223. AAPM, New York.
- Rogers, D. W. O. (1997 (submitted)). . *Med. Phys.*
- Rogers, D. W. O. and Bielajew, A. F. (1986). Differences in Electron Depth Dose Curves Calculated with EGS and ETRAN and Improved Energy Range Relationships. *Med. Phys.* 13: 687 – 694.
- Rogers, D. W. O. and Booth, A. (1996). PROT: A General Purpose Utility for Calculating Quantities related to Dosimetry Protocols. Technical Report PIRS-529, NRC Canada, Ottawa, K1A 0R6.
- Rogers, D. W. O. and Ross, C. K. (1988). The Role of Humidity and Other Correction Factors in the AAPM TG-21 Dosimetry Protocol. *Med. Phys.* 15: 40 – 48.
- Rogers, D. W. O., Ross, C. K., Shortt, K. R., and Bielajew, A. F. (1986). Comments on the  $^{60}\text{Co}$  Graphite/Air Stopping-Power Ratio used in the AAPM Protocol. *Med. Phys.* 13: 964 – 965.
- Rogers, D. W. O., Ross, C. K., Shortt, K. R., Klassen, N. V., and Bielajew, A. F. (1994). Towards a Dosimetry System Based on Absorbed-Dose Standards. IAEA-SM-330/9 in Proc. of Symp. on Meas. Assurance in Dosimetry, (IAEA, Vienna): 565 – 580.
- Ross, C. K. and Klassen, N. V. (1996). Water calorimetry for radiation dosimetry. *Phys. Med. Biol.* 41: 1 – 29.
- Ross, C. K., Klassen, N. V., Shortt, K. R., and Smith, G. D. (1989). A direct comparison of water calorimetry and Fricke dosimetry. *Phys. Med. Biol.* 34: 23 – 42.
- Ross, C. K., Klassen, N. V., and Smith, G. D. (1984). The Effect of Various Dissolved Gases on the Heat Defect of Water. *Med. Phys.* 11: 653 – 658.
- Ross, C. K. and Shortt, K. R. (1992). The effect of waterproofing sleeves on ionization chamber response. *Phys. Med. Biol.* 37: 1403 – 1411.
- Ross, C. K., Shortt, K. R., Rogers, D. W. O., and Delaunay, F. (1994). A Test of  $\text{TPR}_{10}^{20}$  as a Beam Quality Specifier for High-Energy Photon Beams. IAEA-SM-330/10, in Proceedings of Symposium on Measurement Assurance in Dosimetry, (IAEA, Vienna): 309 – 321.
- Schulz, R. J., Almond, P. R., Kutcher, G., Loevinger, R., Nath, R., Rogers, D. W. O., Suntharalingham, N., Wright, K. A., and Khan, F. (1986). Clarification of the AAPM Task Group 21 Protocol. *Med. Phys.* 13: 755 – 759.
- Seuntjens, J., Van der Plaetsen, A., Van Laere, K., and Thierens, H. (1993). Study of correction factors and the relative heat defect of a water calorimetric determination of absorbed dose to water in high energy photon beams. IAEA-SM-330/6 in: Measurement Assurance in Dosimetry. Proceedings of a Symposium, Vienna 24–27 May, 1993 (Vienna: IAEA): 45 – 59.
- Seuntjens, J. P., Shortt, K. R., Ross, C. K., Ma, C. M., and Rogers, D. W. O. (1996). Measurement of beam quality factors  $k_Q$  for cylindrical ionization chambers in high energy photon beams. *Med. Phys.* (abstract) 23: 1071.
- Shiragai, A. (1978). A Proposal Concerning the Absorbed Dose Conversion Factor. *Phys. Med. Biol.* 23: 245 – 252.
- Shiragai, A. (1979). Effective Mass Stopping Power Ratio in Photon Dosimetry. *Phys. Med. Biol.* 24: 452 – 454.
-

- Shortt, K. R., Ross, C. K., Schneider, M., Hohlfeld, K., Roos, M., and Perroche, A.-M. (1993). A Comparison of Absorbed Dose Standards for High Energy X-rays. *Phys. Med. Biol.* 38: 1937 – 1955.
- Spencer, L. V. and Attix, F. H. (1955). A theory of cavity ionization. *Radiat. Res.* 3: 239 – 254.
- Van der Plaetsen, A., Seuntjens, J., Thierens, H., and Vynckier, S. (1994). Verification of absorbed doses determined with thimble and parallel-plate ionization chambers in clinical electron beams using ferrous sulphate dosimetry. *Med. Phys.* 21: 37 – 44.
- Vatnitsky, S. M., Siebers, J. V., and Miller, D. W. (1995). Calorimetric determination of the absorbed dose-to-water beam quality correction factor  $k_Q$  for high-energy photon beams. *Med. Phys.* 22: 1749 – 1752.
- Weinhous, M. S. and Meli, J. A. (1984). Determining  $P_{ion}$ , the correction factor for recombination losses in an ionization chamber. *Med. Phys.* 11: 846 – 849.
- Wu, A., Kalend, A. M., Zwicker, R. D., and Sternick, E. S. (1984). Comments on the method of energy determination for electron beam in the TG-21 protocol. *Med. Phys.* 11: 871 – 872.
-